



**INVESTIGATION OF OPTIMUM FLOW RATE CONDITIONS FOR
PV/T MODULES THROUGH A SIMULATION USING
ECONOMIC TOOLS**

by

Constantinos Faitatzoglou

Strathclyde University
Department of Mechanical Engineering

Glasgow, April 2003

Thesis submitted in accordance with the requirements for a degree
of MSc in Energy Systems and the Environment at the University of
Strathclyde

DECLARATION OF AUTHOR'S RIGHTS

The copyright of this thesis belongs to the author under the terms of the United Kingdom Copyright Acts as qualified by the University of Strathclyde Regulations 3.49. Due acknowledgement must always be made of the use of any material contained in, or derived from, this thesis.

ABSTRACT

Photovoltaic generation is the direct conversion of solar energy to electricity, and arises from separating positive and negative charge carriers in an absorbing material. This form of energy generation is not competitive due to a combination of factors including materials and manufacturing costs and low conversion efficiency (usually around 15% for high efficiency commercial cells). One additional drawback with photovoltaic technology is that a cell's efficiency is inversely proportional to the heat it absorbs; for every degree Kelvin of temperature increase there is a corresponding decrease in cell efficiency. By adding a heat recovery system, fed with air or water, a temperature reduction to the cell can be achieved, while the heat transferred can be used in space or water heating. This modification creates a hybrid system of solar-thermal and solar-electrical generation.

This project aims to create a process to identify the optimum flow rate (\dot{m}) of such a hybrid system. This will balance the characteristics that govern the system's energy output, increasing its efficiency and generation ability and aiming to give it an added value. Concurrently simulations identifying optimum flow rate variations with respect to different weather conditions will also be analyzed.

ACKNOWLEDGMENTS

First of all I would like to express my thanks to Dr. Nick Kelly for supervising this project. I would also like to thank my parents for their continuing support and the 2001/02 residents of M329 for all the fun and enjoyable moments we shared.

TABLE OF CONTENTS

Introduction	
Overview	1
Scope and aims of this study	2
Chapter 1	
Hybrid PV/Thermal collectors technology review	4
The photovoltaic/thermal (PV/T) concept.....	4
Technology status and literature review	5
Glazed and unglazed systems.....	5
Water and Air	6
Insulation and PCM	11
Heat Pumps.....	12
Economic aspects	13
Conclusion	14
Chapter 2	
Developing a model.....	16
Thermal network	16
Heat loss coefficients.....	19
Heat removal factor	20
The model	22
Simulation Process.....	24
Weather data	24
Weather data polynomials.....	24
Daily energy outputs.....	25
Relating the energy outputs with F_R	26
Relating the flow rate to the heat removal factor.....	27
System's surcharge due to water pumping	31
Energy yield and application of economic tools.....	32
Conclusions	33
Chapter 3	
Validation	35
Chapter 4	
Simulation and analysis	36
System configuration analysis.....	36
High latitude results.....	36
Central latitude results	39
Low latitude results.....	42
Parametric analysis	45

Conclusions	48
Chapter 5	
Discussion of Results and Conclusions	49
Discussion	49
Summary of conclusions	54
Areas for further study	54
Conclusions	55
Nomenclature	
Bibliography	
Appendixes	

INTRODUCTION

Overview

The world's deliberations concerning global warming and the significant impact that the conventional energy production technologies made to the environment, turned the attention of our society to alternative energy resources. Alternative energy technologies harness the natural reserves, promote sustainability and a better equilibrium between human prosperity and the environment. Since the majority of these resources are neither constant nor predictable and with limited efficiency tolerance, it is often necessary to use two or more of these technologies, forming a hybrid system.

Hybrid energy systems combine the use of two or more alternative power sources and aim to increase the system's total efficiency. The photovoltaic/thermal (PV/T) system is a hybrid structure that has been examined quite thoroughly over the past years and makes use of the 70%-95% of collected solar energy that is not converted into electricity by conventional solar cells.

Photovoltaic (PV) cells have been introduced a few decades ago and were used initially for supplying energy in spacecraft and satellites. Once commercialized, in the 80's, their price was too high to be considered as a competitive source of energy. Though, the market's aim was to find ways for cheaper cell manufacturing procedures, cheaper materials and higher efficiency, so that the energy production from solar cells to become more competitive. They achieved that by reducing this cost by 75% over the last 20 years [1].

One of the main drawbacks with photovoltaic technology is that the modules efficiency is inverse proportional to the heat they acquire. As seen in Figure 1¹, this is more significant in higher efficiency modules (mono-crystalline) where for every Kelvin (or °C) of temperature increase there is about half percent decrease in cell efficiency. To eliminate this problem several hybrid system configurations have been investigated. A heat recovery medium, air or water, is used to decrease the modules

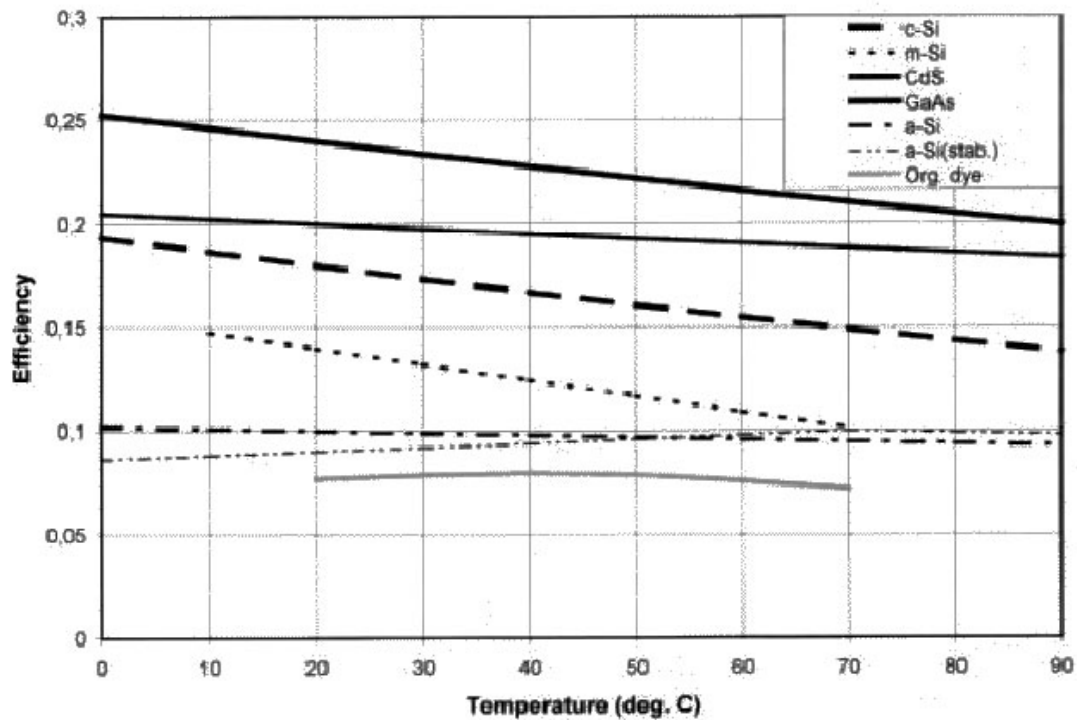


Figure 1: Solar cell efficiency as function of operating temperature, normalized to typical 25°C (B. Sorensen, 2000)

temperature and uses the acquired heat for operations such as area heating, natural ventilation, or hot tap water supply.

For locations with low ambient temperatures (high latitude countries), where space heating is necessary for almost all of the year, PV cooling by air circulation can prove to be more cost effective and useful. On the other hand, in areas with high solar input and ambient temperatures (low latitude countries) liquid PV cooling can be the most promising solution.

Scope and aims of this study

Previous studies in this area have been trying to identify the potential that a PV/T system has, and the parameters that govern this system, such as solar insolation, ambient temperature, wind velocity and inlet temperature (either using a liquid or air as the heat recovery medium). This project aims to create a process to identify the optimum flow rate (\dot{m}); this will balance the characteristics that govern the system's energy output, increasing its efficiency and generation ability. Using that process, the parameters that affect the optimum conditions will

be assessed to determine how the optimum flow rate varies with latitude. To achieve that, economic tools will be used.

¹ B. Sorensen "PV power and heat production: an added value" Proceedings of the 16th European Photovoltaic Solar Energy Conference in Glasgow, 2000

CHAPTER 1

Hybrid PV/Thermal collectors technology review

The photovoltaic/thermal (PV/T) concept

The solar radiation which is produced from the sun, gives a resulting average flux incident on a unit area perpendicular to the beam of 1367 W/m^2 . This power received per unit area and called irradiance, is reduced once entering the earth's atmosphere by air molecules, clouds and aerosols. The degree to which attenuation occurs, and is about 30% of the extraterrestrial intensity, is a function of the number of particles through which the radiation passes and the size of the particles relative to the radiations wavelength, λ .

Part of the solar radiation can be converted in electricity by the photovoltaic effect and part of it to thermal energy. In Figure 2 a smoothed graphical representation of the solar radiation is demonstrated. The shaded part (B) represents the photon energy converted to electrical energy whilst area C corresponds to the excess photon energy that is wasted as heat. Area B radiation, which is greater or equal to the band gap energy of a silicon material, sets free electrons from the solar cells atomic bond creating electron-hole pairs generating a photoelectric current.

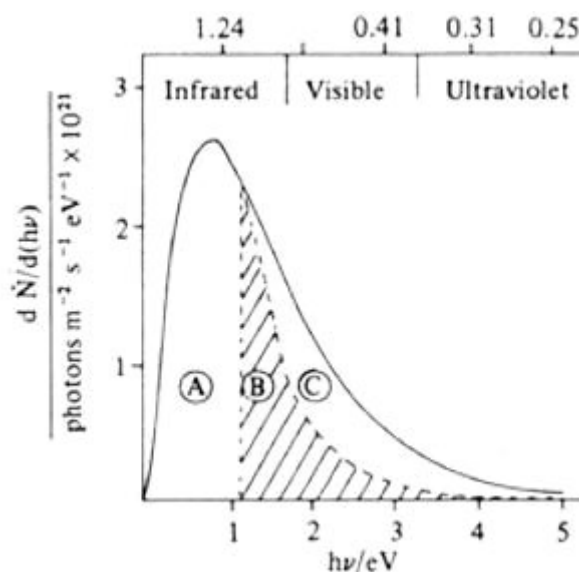


Figure 2: Solar radiation with AM1 (Twidell & Weir, 2000)

The photovoltaic/thermal concept is a combination of a solar heat collector with photovoltaic cells placed on the top, forming a hybrid system that generates low grade heat and electricity. The radiant energy from the sun is partly converted to electricity by the photovoltaic cells that

are in thermal contact with a solar heat absorber, and the excess heat generated in the cells serves as input for the thermal system. Apart from the fact that this hybrid configuration can give a high conversion efficiency system, it can contribute to increase the performance of the PV cells since it is well known that the excess heat absorbed decreases their efficiency by approximately 0.5% for every extra degree Celsius.

Technology status and literature review

PV/T systems are distinguished by the heat recovery mediums used (air and water) to utilize the thermal gain and increase of the cell's performance. Usually they are structured as PV cells placed on the top of an absorbing plate that is connected to an air duct or water pipes. The front side is either exposed to free convection or glazed to improve the thermal performance of the system. The backside is either insulated, or filled with phase change materials (PCM) that act as a latent heat storage system to store the excess thermal energy and deliver it later on the day. Finally, heat pumps can be combined with these modules to give an additional value to the system.

The results of the aforementioned combinations rely on a variety of parameters. These can be the geographic area, the system orientation and the relating weather conditions, the material used for the photovoltaic cell (as it is comprehended from Figure 1), the mass flow rate of water or air, and, most of all, the reason behind the use of the system.

Glazed and unglazed systems

Even though the gap that needs to be covered for the electrical efficiency seems to be small, the one for the thermal efficiency is rather bigger and easier to control according to the current technology. By adding an extra glazing area with an air gap between the PV and the glazing reduction in thermal losses with a small deficit in the electrical efficiency can be achieved.

Unglazed PV systems are used in plain electricity systems where the ambient air acts as the coolant medium and cools down the module by convection from the front and back side without recovering any of the heat; such an action in a hybrid system, equates to a lot of thermal losses

to the ambient. An extra glazing layer reduces the irradiance that reaches the PV panel, decreasing the performance of the module, the thermal gain though from that extra layer overcomes that small deficit.

These aspects were studied by Tripanagnostopoulos *et al.*(2002)² who investigated various component combinations for optimum performance. Components like booster diffuse reflectors (Figure 3) and glazing layers are added to plain PV panels, while air and water is used to investigate the system which is the most promising in performance.



Figure 3: PV/T system with booster diffuse reflectors (Tripanagnostopoulos *et al.*(2002))

Moreover in the glazing aspect, an increase up to 30% in the thermal efficiency was determined while in the electrical efficiency a reduction due to optical losses of 16% (to that of the basic, no glazing, PV/T system) was found. By combining a glazing layer with a booster diffuse reflector the results gave a 45% (using water) and almost a 100% (using air) increase of thermal output compared to that of the basic PV/T. On the contrary, the electrical output got balanced to the unglazed system (meaning that there was a 16% increase of solar energy to each module because of the reflectors).

Water and Air

The most common heat recovery mediums of the PV/T systems are air and water. Relevant works by scientists, which have been undertaken in the past few years, have been proved that the calculated thermal efficiencies of liquid type PV/T systems range between 45% and 65%. The higher values derived from systems that use air gap with glazing for thermal losses suppression. Regarding air type PV/T systems, thermal efficiencies up to about 55% are given by theoretical models for long systems with a small air duct.²

The two aforementioned media have totally different thermodynamic characteristics and properties. The product $\rho \cdot C_p$ (ρ is the density and C_p the specific heat) is commonly termed as the volumetric

heat capacity and measures the ability of a material to store thermal energy. Liquids, because of their large density, are typically characterized as good energy storage media while gases are poorly suited for that. For air at 25°C and at atmospheric pressure, density is 1.16kg/m³ and the specific heat is 1007 J/kgK; water at the same conditions has density equal to 996 kg/m³ and specific heat equal to 4179 J/kgK.

In a similar vein the heat transfer characteristics are different. The thermal diffusivity, $\alpha = \frac{k}{\rho \cdot C_p}$, is defined as the property that measures the ability of a material or substance to conduct thermal energy relative to its ability to store it. Substances with large values of α , have the ability to respond faster to changes in their thermal environment, while substances with small thermal diffusivity respond sluggishly and are better storage media. For air at 25°C the thermal diffusivity value is 22.5m²/s whilst for water is 0.147m²/s. It is obvious that it is more efficient to use air for direct applications and water for energy storage. In the study of Tripanagnostopoulos *et al.* (2002)², it has been noted that heat extraction by water circulation is more efficient than that of air circulation.

Various analytical models have been created to simulate the performance and test new design parameters. Most of them are based on the Hottel - Whillier model for thermal analysis of the flat plate collector

$$Q_{net} = \tau_{glaze} \alpha_{plate} A_{plate} G - U_L (T_p - T_a) \quad (1.1)$$

and extended to the analysis of combined PV/T collectors. Amongst the first who attempted such an approach was Florschuetz³ who assumed that the electrical conversion efficiency of the solar cell is a linear decreasing function of the absorbers operating temperature

$$\eta = \eta_r [1 - \beta_r (T - T_r)] \quad (1.2)$$

where η is the efficiency, β the cell's efficiency temperature coefficient and r represents the reference values. Assuming the temperature gradients across the absorber thickness negligible, he derived an expression representing the electrical output in relation to the ambient temperature, the collector fluid inlet temperature, the intensity of incident sunlight and the above mentioned cell parameters:

$$Q_e = \frac{A_c S \eta_a}{\alpha} \left\{ 1 - \frac{\eta_r \beta_r}{\eta_a} \left[F_R (T_{f,i} - T_a) + \frac{S}{U_L} (1 - F_R) \right] \right\} \quad (1.3)$$

Moreover, Bergene and Lovvik (1995)⁴ gave a detailed analysis of the energy transfer between the different components of a liquid PV/T system with results for electrical and thermal efficiencies. They also noticed that the energy output is very promising since the system's energy density is increased (W/m²). This model was based on Duffie's and Beckman's⁵ flat-plate solar heat collector model and assumed steady state conditions. Two significant expressions were derived from this study; the water temperature as a function of the tube length:

$$T(y) = T_a - \frac{q(T_a)}{q'(T_a)} - \left(T_a - T_i - \frac{q(T_a)}{q'(T_a)} \right) \exp\left(\frac{q'(T_a) \cdot y}{\dot{m} \cdot C_p} \right) \quad (1.4)$$

and the average solar cell temperature:

$$\bar{T}_s = \frac{1}{LW} \left(2 \int_0^L dy \int_0^{\frac{W-D}{2}} dx T_{sf}(x, y) + D \int_0^L dy T_s(y) \right) \quad (1.5)$$

In these expressions, $q(T_a)$ is the generated heat, T_s represents the solar cell temperature above the tube and T_{sf} at the fin (the area between two consequent tubes), assuming that the silicon cell and the copper (usually) plate are very thin, and there is no temperature variation in the thickness.

Apart from the steady state mathematical representation of a PV/T, the above mentioned study notes the importance of the flow rate and the inlet fluid temperature for the electrical and thermal performance of the system. When the flow rate is around 0.001kg/s, it is noted that there is not much to gain, thermodynamically, on increasing it further and at low flow rates the electrical efficiency increases when the tubes have small diameter. This occurs because a small tube diameter will give a higher fluid velocity inside the tube, decreasing the outlet temperature T_L , and giving a corresponding increase in the solar cell's efficiency. Regarding the theoretical performance of these systems the authors claim that a relative increase of 10% to 30% is noted in the solar cells efficiency as the result

of cooling and the total photovoltaic/thermal efficiency can achieve values between 50% and 80%.

Sandnes and Rekstad (2002)⁶ analyze a system which uses square plastic channels filled with ceramic granulates (Figure 4) to increase the heat transport from the absorber to the heat carrier fluid. While creating an analytical model for the system, they spotted clearly how important is the liquids inlet temperature for a high performance PV operation. The benefits of a square, wall-to-wall, fluid channel that covers the entire back side of the absorber and has a fin efficiency of 1, were spotted in the increase of power, as it was found equal to 8.8% compared to a system without fluid circulation. The authors also note that the effect of extracting electrical power from the solar cells is a corresponding reduction in the solar energy available for the thermal system; when the system was disconnected from the circuit an increase on the thermal output equal to the previous power output was determined. In addition, it is noted that the inlet fluid temperature is the main reason of the cooling effect and a relation between that and the cell temperature was validated

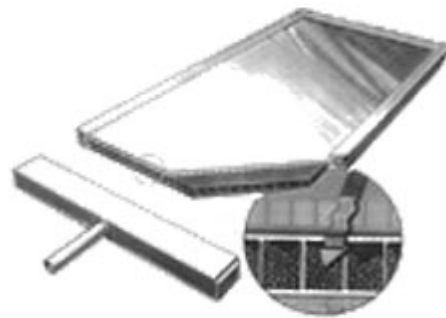


Figure 4: SolarNor collector with ceramic granulates

$$T_{pv} = T_i + \frac{1 - F_R}{F_R U_L} \eta_T I \quad (1.6)$$

where T_i is the inlet water temperature, F_R the heat removal factor, U_L the overall heat loss coefficient, I the solar radiation and η_T the thermal efficiency.

Regarding systems with air as the heat recovering medium a few modeling solutions have been reported as well. Lee *et al.*⁷ have developed such a simulation for Borland Delphi and concluded that the model could provide a reasonable first approximation for predicting the PV temperature (and its efficiency in extend), while the outlet temperature results were not satisfactory and more work needs to be done on that. Nevertheless,

Evans and Kelly⁸ derived equations for PV power output and façade recovered heat, which were incorporated in the ESP-r building simulation platform.

Finally, Krauter *et al.*⁹ performed experiments on four PV façade configurations, a PV/T with water circulation (HYPTIVE), two PV/T with air as the heat recovery medium (one with natural convection and the other with forced convection) and a PV insulated on the back (TIPVE). After

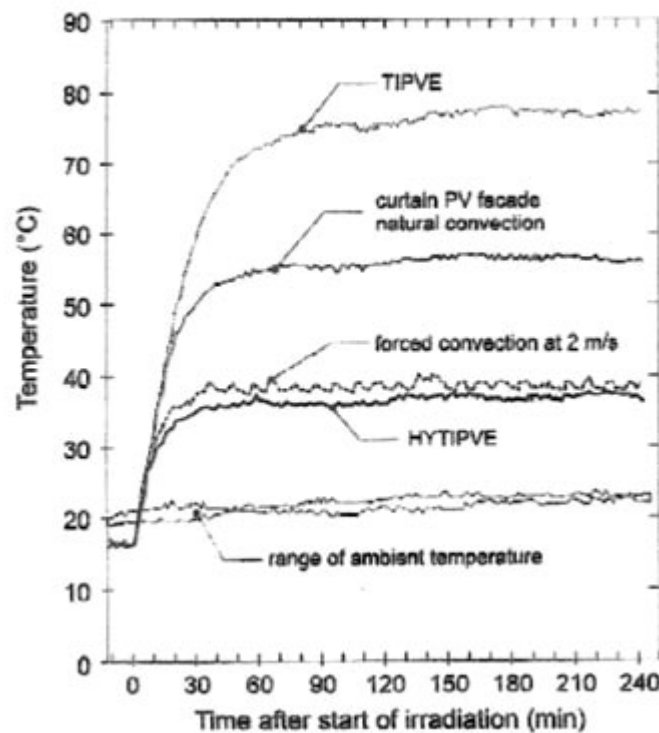


Figure 5: Temperature as a function of time for different PV façade configurations ($G=700\text{W}/\text{m}^2$) (Krauter *et al.* 1999)

collecting the data from the experiments, he used steady state energy flux relationships to calculate the thermal energy delivered by each component. Figure 5 illustrates the measured PV temperature as a function of time. For the HYPTIVE model with mass flow rate of 47.7gr/sec a heat flux of $379.2\text{W}/\text{m}^2$ for the water was found while for the forced convection (2m/s) experiment the result was a flux of $164.3\text{W}/\text{m}^2$. It is worth mentioning that the back insulated PV had a heat flux, to the front of the panel equal to $393.2\text{W}/\text{m}^2$. The increase of the PV performance for the forced convection system is 8% and for the water circulation system

9%, while a decrease of 9.3% was found for the thermal insulated PV façade (all values are relative to the conventional PV façades).

Insulation and PCM

Two important factors about the performance of a hybrid PV system are the thermal losses and the PV module temperature. The aim is to keep the silicon compound to a temperature as low as possible while there is not any heat losses. In PV/T systems this can be achieved by significantly reducing the back loss coefficient (U_b from Duffie and Beckman⁵). Usually an insulating material, like fiberglass, is used while the heat is recovered immediately by the working fluid; air or water. Alternatively you can accommodate the properties of phase change materials (PCM) and achieve a demand shift.

Phase change materials can store a high amount of thermal energy

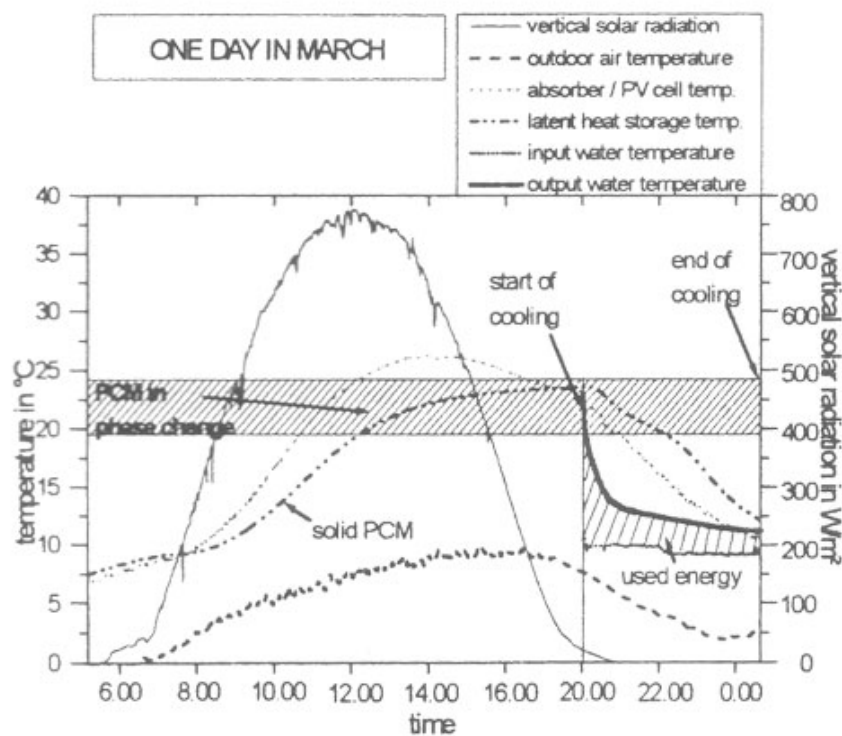


Figure 6: Temperature curves for the PCM module (Haeusler et al., 2000)

in a small volume. That is reached by using the effect of energy storage during the phase change from the solid to the liquid phase while there is an output of that stored energy in the change from the liquid to the solid phase.¹⁰ Tobias Haeusler *et al.* (2000) have performed experiments on

hybrid PV facades with latent heat storage where the heat was stored throughout the day and extracted after the dusk (Figure 6). The paraffin wax had a phase change temperature of 24°C and achieved a 15% to 30% increase in the electrical power in comparison to the plain PV facades and a total of 120Wh were gained throughout the test day. In addition to that 1.05 kWh of thermal energy was gained from the system from which 51% was from the melting of the PCM. The study does not include economic aspects.

Heat Pumps

The need to extract heat to a higher temperature has been proved to involve a reduced efficiency in the electricity production of the high performance photovoltaic cells. With the addition of a heat pump it is feasible to increase the performance of the system by collecting heat at temperatures around 20°C and delivering it at around 50°C. These systems involve an additional cost due to the equipment and the electricity required to drive the heat pump. With a coefficient of performance (COP) of 3 to 4 for many current heat pump systems, the power required is $\frac{\text{amount of heat treated}}{COP}$ ¹. The simple solar thermal

system can achieve efficiencies up to 80%, but at the same time diminishes that to less than a half by the need for storage if considered for more than summer hot water supply. The solar cell plus a heat pump system offers an efficiency of η_{th} times COP minus the storage losses which are typically much less than for heat systems¹.

Leenders *et al.*(2000) refer on two PV thermal heat pump systems, one with an air collector and one with a water collector. The first one (Figure 7) is demonstrated in Zwaag, Netherlands and simply upgrades the preheated air to low temperature space heating while a heat recovery

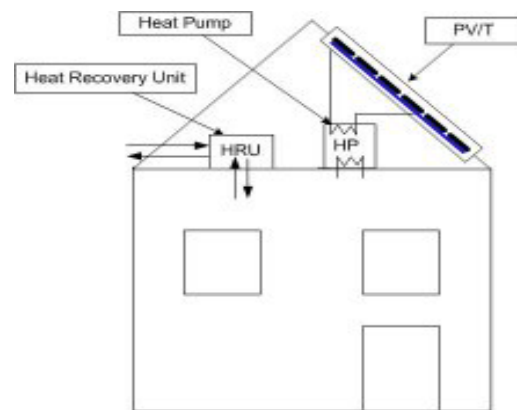


Figure 7: PV/T air collector combined with a heat pump and a heat recovery unit

unit is installed to reduce the heat losses. The second deals with the aquifer; in the summer the PV/T is cooled down with water from the aquifer to provide higher power output. While cooling the PV/T, the water is heated to about 20°C, and stored in the aquifer to be used during the winter. In winter the heat pump upgrades the stored heat in order to provide low temperature space heating of about 40°C¹¹. According to the authors the latest concept offers opportunities to regenerate the heat in the soil when heat pumps are used on a large scale in urban areas.

Economic aspects

Using today's technology a hybrid thermal system yields less energy than the sum of the separate components. The cost though of two solar systems, one for power and one for heat, should be higher than that of any combined power and heat system due to common components. Leenders *et al.*¹¹ and Sorensen¹ performed some basic economic

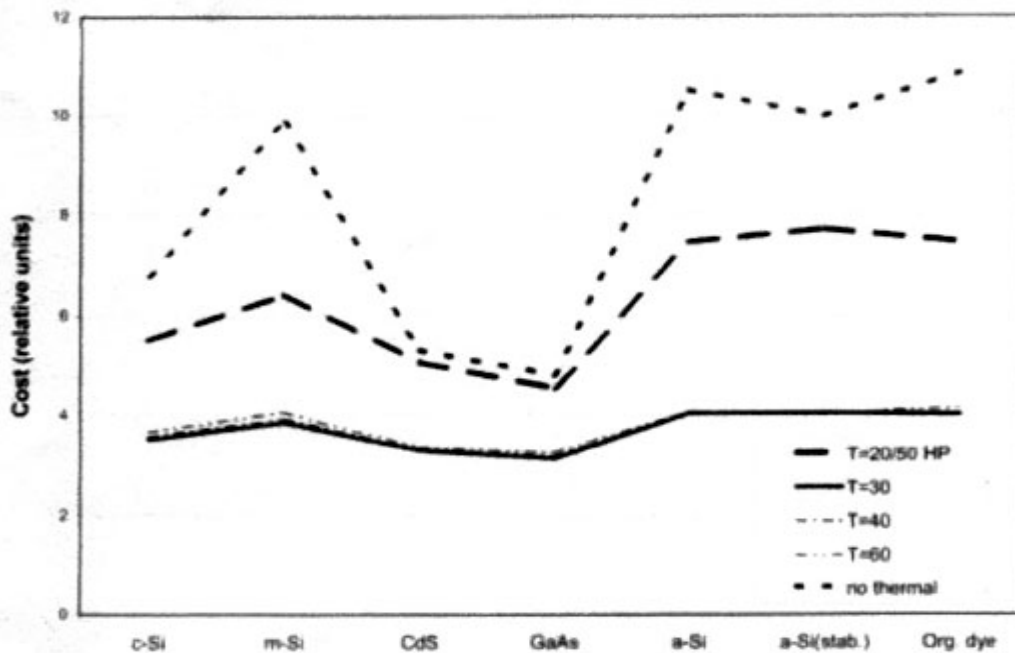


Figure 8: Relative cost of different PV/T systems (Sorensen, 2000)

comparisons between a variety of PV/T systems. The first paper reports system costs, electricity and gas savings for the central European countries while the second one compares the different combined solar power systems to the cost of a pure electricity system (Figure 8). Leenders *et al.* give estimations for two water PV/T systems. The first one

is without storage (for outdoor swimming pool heating) and has installation cost (for a polycrystalline panel) of €560/m², electricity saving of €8.5/m²yr and gas savings of €5.5/m²yr. The second one has a storage tank for tap water and installation cost of €865/m², electricity savings of €7.5/m²yr and gas savings of €7/m²yr. Regarding the heat pump systems the most economic seems to be the one with the heat recovery unit with installation cost of €730/m² and electricity savings of €8/m²yr.

Conclusion

In this literature review the concept of the photovoltaic/thermal system was examined to its current state in industry and research. Information relevant to the aspects which affect such a module was obtained, and validated assumptions with mathematical representations, that will aid the approach to this study's objectives, were quoted. It was also discovered that, so far, there is not any study conducted on a methodology to determining the optimum flow rate of a PV/T module's heat recovery medium.

² Y. Tripanagnostopoulos, Th. Nousia, M. Souliotis and P. Yiannoulis "Hybrid PV/T Solar Systems" Solar Energy, Vol. 72, No3, pp217-234, 2002

³ Florschuetz, L.W. "Extention of the Hottel-Whillier model to the analysis of combined Photovoltaic/Thermal flat plate collectors" Solar Energy Vol. 22, pp.361-366, 1979

⁴ T. Bergene and O. Lovvik "Model calculations on a flat-plate solar collector with integrated solar cells" Solar Energy, Vol. 55, No. 6 pp 453-462, 1995

⁵ Duffie, J., Beckman W. "Solar engineering of thermal processes" 2nd ed., Wiley and Sons, 1991

⁶ B. Sandnes and J. Rekstad "A PV/T collector with Polymer absorber plate. Experimental study and analytical model" Solar Energy Vol. 72, No 1 pp 63-73, 2002

⁷ Lee, W. M., Infield, D. G., Gottschalg, R. "Thermal modeling of building integrated PV systems" REMIC, 2001

⁸ Evans M, Kelly N "Modeling active building elements with special materials" ESRU, Strathclyde University, Glasgow 1996

⁹ Krauter, S, Araujo, R.G., Schroer, S., Hanitsh, R., Salhi, M.J., Triebel, C., Lemoine, R. "Combined photovoltaic and solar thermal systems for façade integration and building insulation" Solar Energy Vol. 67, pp. 239-248, 1999

¹⁰ Haeusler, T., Rogass, H. "Latent heat storage on Photovoltaics" 19th European PV solar energy conf., Glasgow, 2000

¹¹ Leenders F., Schaap A.B., van der Ree B.G., van der Helden W.G.J. "Technology review on PV/Thermal concepts" 19th European PV solar energy conf., Glasgow, 2000

CHAPTER 2

Developing a model

Thermal network

In order to assess the optimum flow rate, it is essential to create a mathematical model of the photovoltaic/thermal system. The mathematical model will be based on existing validated assumptions and formulas.

The thermal network illustrated in Figure 9 represents a PV/T system. Someone can realise the similarity of such a system to the

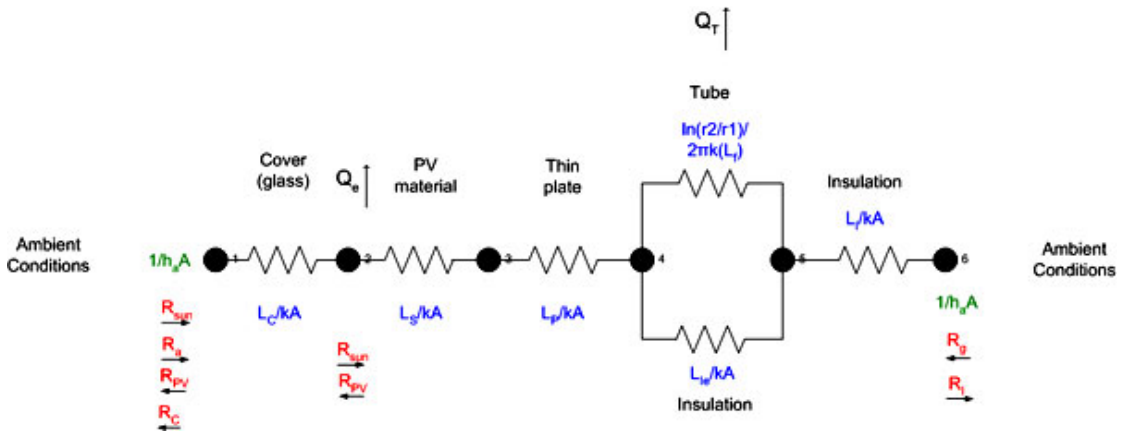


Figure 9: Nodal network of a PV/T system

thermal one analyzed by Duffie and Beckman⁵. The differences are concentrated in the power extraction, Q_e , and the extra layer of the PV material on the absorbing plate. Q_e is the power generated by the PV panel (Florschuetz (1978)),

$$Q_e = \eta_{PV} \cdot \frac{S}{\alpha_{PV}} \cdot A \quad (2.1)$$

where η_{PV} is the PV incident efficiency, α_{PV} is the absorptance of the module (usually taken between 0.8 and 0.9), S is the absorbed solar radiation, and A is the area.³ Regarding the extra silicon layer on the absorber, Florschuetz (1978) and Sandnes *et al.* (2001) suggest taking the average thermal conductivity, k , value of the silicon material and the plate, weighted according to the cross-sectional areas of the cell and plate.

In a similar way as Duffie and Beckman did for the thermal absorbing plate, to evaluate the system, it will be easier to reduce the parameters, so, the above nodal system is reduced to the one shown in Figure 10, adapting at the same time the assumption and formulas they derived. Sandnes *et al.*(2001) based their analytical model on this procedure and the simulation results they derived were in agreement with the experimental data.

The steady state energy balance equation for the system is:

$$Q_T = A_c F_R \left[\dot{S} - U_L (T_i - T_a) \right] \quad (2.2)$$

where A_c is the collector's area, \dot{S} is the solar energy available for the thermal system, which is equal to:

$$\dot{S} = \left((\tau\alpha) - \eta_{PV} \frac{A_{pv}}{A_c} \right) I \quad (2.3)$$

F_R is the heat removal factor as defined by Duffie and Beckman; the quantity that relates the actual useful energy gain of a collector to the useful gain if the whole collector surface were at the fluid inlet temperature. A_{pv} is the area covered by the photovoltaic cells.

$$F_R = f(\dot{m}_w, U_L, tube \text{ geometry}) \quad (2.4)$$

Depending on the liquid heater design the formula takes different forms. The loss coefficient, U_L , is the sum of the top loss coefficient, U_{top} , and the back loss coefficient, U_{back} . Moreover, T_i and T_a represent the inlet and ambient temperature respectively.

If there is a storage tank for the system, the useful energy will be:

$$Q_u = Q_T - Q_{tank} \quad (2.5)$$

with

$$Q_{tank} = (UA)_{tank} (T_w - T_a) \quad (2.6)$$

where T_w is the storage fluid temperature. The storage fluid temperature can be equal to the average outlet temperature if we supply the system with cold tap water all the time (Figure 11b) or to the inlet temperature, if a water circulation system (Figure 11a) is used. A fully mixed storage

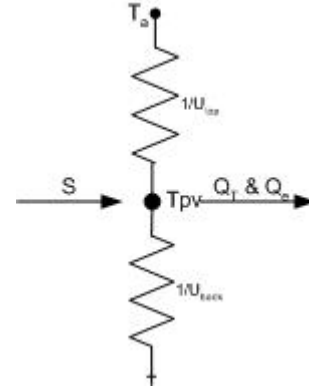


Figure 10:
Equivalent
thermal network
for the PV/T

tank is assumed in this model, since to benefit from a stratified tank we need low flow rates that will not promote the cooling of the PV module. The second case in Figure 11 can be expressed as

$$mC_p \frac{dT_w}{dt} = A_c F_R [S(t) - U_L (T_i - T_a(t))] - (UA)_{tank} (T_w(t) - T_a(t)) \quad (2.7)$$

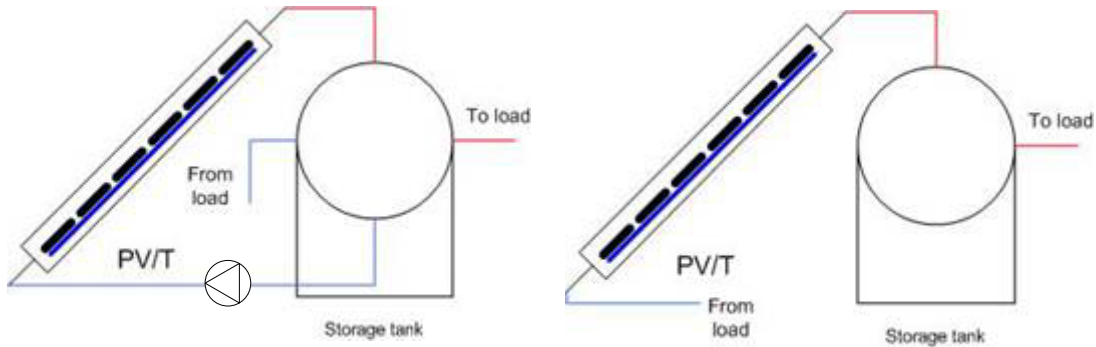


Figure 11: PV/T system configuration

For the first case T_i equal to T_w is used. The value m is the fluid mass in the system.

Tank stratification is the result of the fact that the density of fluids is a function of temperature and that decreasing density occurs with increasing temperature. In other words, fluids in tanks will tend to stratify with the hotter fluid on top of the colder. Stratification in a tank depends on the flow rate and temperature of incoming fluid streams alongside the design of the storage tank. Low flow rates mean less convective mixing, which causes loss of stratification in a tank.

Another reason for loss of tank's stratification is the "plume entrainment"¹² phenomenon. According to Kleinbach *et al.*(1993) this occurs in the late afternoon or during a cloudy period when the availability of solar energy has decreased and the incoming water may be

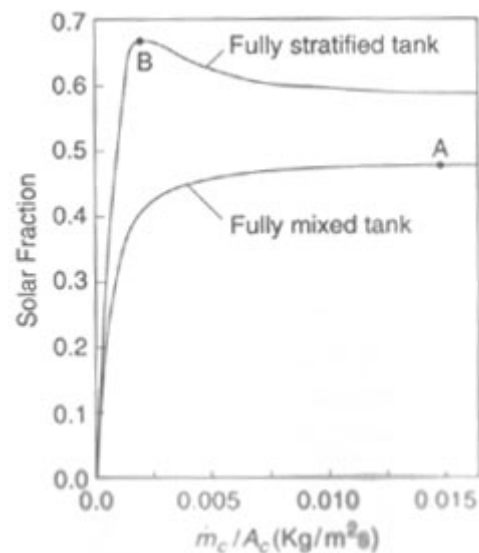


Figure 12: Example of optimum flow rates for stratified and mixed tanks (Wusteling *et al.*(1985))

cooler than the upper portion of the tank which is still hot due to higher energy input earlier in the day. This causes the hot fluid already in the tank to be entrained in the falling plume and fall down to a higher density level, laying off its temperature.

In high latitudes, where the irradiation is low along with the ambient temperature, low flow rate systems are often used to utilize any available energy. In such systems the system's flow rate should be in a specific range of values, since, as can be noted from Figure 13, outside this range the thermal performance decreases rapidly.

Heat loss coefficients

The back loss coefficient, U_{back} , is a function of the insulation material properties and its thickness, while the top loss coefficient includes radiation, convective and conductive losses.

For systems that use glass as a cover and no infrared radiation passes directly through the cover, the top loss coefficient can be expressed as

$$U_{top} = \left(\frac{1}{h_c + h_{r,in}} + \frac{1}{h_{wind} + h_{r,a}} \right)^{-1} \quad (2.8)$$

where h_c is the convection heat transfer coefficient between the two parallel plates, $h_{r,in}$ is the radiation heat transfer coefficient between them, h_{wind} is the convection heat transfer coefficient that is relative to the wind, and $h_{r,a}$ is the radiation heat transfer coefficient from the cover plate to the ambient.

Plastic glazing covers, which allow the infrared radiation to heat the system, are usually not used in PV/T systems due to the substantial losses in power from the decreased direct solar radiation that reaches the PV.

An alternative configuration is to have an extra layer of glass attached to the top of the PV panel for protection. This layer is about 4mm thick and glued with resin (1mm thick) on the top of the silicon PV material. Consequently, the top loss coefficient becomes:

$$U_{top} = \left(\frac{1}{h_{k,glass} + h_{k,resin}} + \frac{1}{h_{wind} + h_{r,a}} \right)^{-1} \quad (2.9)$$

The heat loss from the hybrid PV/T system to the outside winds is important since their value can significantly affect both, power and thermal performance. Duffie and Beckman recommend the use of the experimental results from McAdams and Mitchell for free and forced convection. Data results for free convection for hot inclined flat plates facing upwards are not available and there is no Nusselt number expression for that. Alternatively McAdams recommends the use of $h_{wind} = 5W/m^2K$ for still air conditions, whilst experimental results from Mitchell show that forced convection conditions over buildings can be expressed as

$$h_{wind} = \frac{8.6 \cdot V_{wind}^{0.6}}{L_{plate}^{0.4}} \quad (2.10)$$

The photovoltaic panel's temperature can be assumed equal to the temperature of the absorbing plate of a thermal system which according to Duffie and Beckman is

$$T_{PV} = T_i + \frac{1 - F_R}{F_R U_L} \frac{Q_T}{A_c} \quad (2.11)$$

Having the thermal efficiency as

$$\eta_T = \frac{Q_T}{A_c \cdot I} \quad (2.12)$$

the equation (1.6) is derived from here. This value will be used to evaluate the PV performance as the electrical efficiency is a decreasing linear function of its temperature:

$$\eta_{PV} = \eta_{ref} - \mu(T_{PV} - T_{ref}) \quad (2.13)$$

with μ taking the value of 0.05%/K for single-crystal silicon cells¹³.

Heat removal factor

The heat removal factor is the feature that signifies the performance of the system. It is directly related to the energy that will be acquired by the water, and affects the performance of the silicon cell (due to its appearance in equation 2.10). Quantitative is equal to

$$F_R = \frac{\dot{m}C_p}{A_c U_L} \left[1 - \exp\left(-\frac{A_c U_L F'}{\dot{m}C_p}\right) \right] \quad (2.14)$$

with F' being the collector efficiency factor that varies according to the

design. For a sheet and tube design, like the one in Figure 13, the collector efficiency is

$$F' = \frac{1}{\frac{1}{F_{WD}} + \frac{U_L}{U_{fin}}} \quad (2.15)$$

where F_{WD} is a relation for the tube geometry and U_{fin} the thermal conductance between the absorber and the fin. In addition the bond conductance, C_b , has to be assumed very large. For a wall-wall design the F_{WD} factor is equal to unity and this result to an increased system performance.

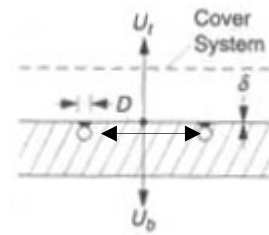


Figure 13: Sheet and tube design

Similarly, there are designs with serpentine tube arrangement which can be represented by a formula from Zhang and Lavan¹⁴. The serpentine system, like the one used by Krauter *et al.* (1999)⁹ will create "hot spots" to the power system, and the power output of each cell will be equal to the one that performs the worst. To avoid this problem the system should have bypass diodes in each cell in which case the average power of the cells will be equal to the total power output of the module.

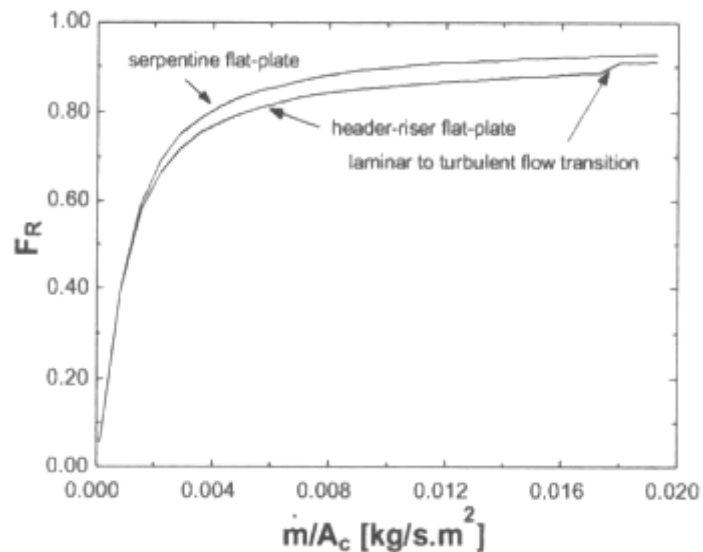


Figure 14: Comparison of the heat removal factor for the single sheet and tube configuration and an 18 bend serpentine system (Dayan *et al.* 1998)

Serpentine tube arrangement tends to increase the performance of a system just because of the higher heat transfer coefficient.¹⁵ This is the result of the higher flow through each riser creating turbulence in less tube distance than a plain sheet-and-tube configuration with the same flow rate. In other words serpentine configuration can be useful in a low flow rate system (around

0.004kg/m²s) that utilizes the turbulent flow and the stratified storage tank. In serpentine configuration systems a minimum value of F_R occurs with one bend ($N=2$) and the maximum value with no bends ($N=1$). This is also noted by Zhang and Lavan¹⁴; as $N \rightarrow \infty$, F_R tends to equal the value of F_R at $N=1$.

The model

The model was built on MathCAD¹⁶ and VisSim PE¹⁷ computer packages. It is a steady state model and the optimum flow rate represents the constant rate that the fluid should have throughout the day. The use of a dynamic model would have been better, however none was found to be validated.

The process of building the model is based on the following idea: The weather data is filtered and polynomial functions are derived to represent the solar intensity and ambient temperature. These functions are “plugged in” equation (2.7) to derive the daily energy gains (electrical and thermal energy). By altering the heat removal factor, F_R , a linear relationship between that and the energy gains is developed. The heat removal factor can be related to the flow rate using the steady state assumptions discussed by Duffie and Beckman⁵. Combining these two relationships, a representation between the flow rate and the energy gains is generated. Subtracting from this relation the energy surcharge due to pumping, a final, total, energy gain can be assessed. By applying economic weighs, depending on the source of energy, to this final step, a maximum is obtained which represents the maximum economic benefit of the system. The flow rate at which this maximum occurs is the optimum flow rate.

The block diagram in Figure 15 shows the steps that were followed and in the appendix the analytical representation of these steps is illustrated. An explanation of each step follows the block diagram.

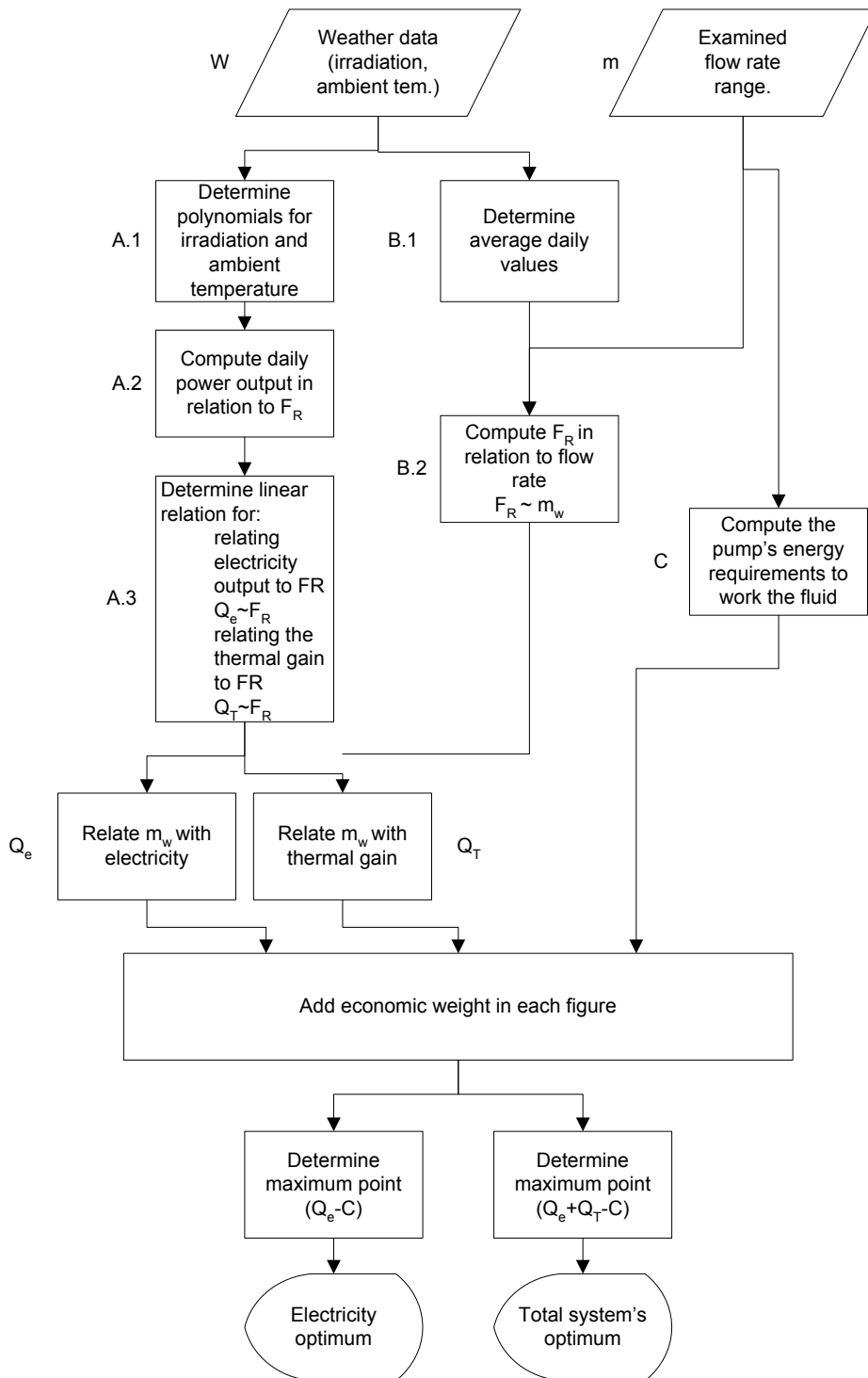


Figure 17: Simulation process block diagram

Simulation Process

Weather data

The data used was taken from the ASHRAE internet site. Two twenty-four hour samples were chosen for each examined city; one representing a clear sky (sky-cover-opacity=0) winter day, and one representing a clear sky summer day. The selected cities were Oslo, Brussels and Thessaloniki.

While the ambient temperature data was taken selfsame, the irradiation data was converted from horizontal to inclined (at the city's latitude) using the isotropic sky diffuse model⁵. The isotropic diffuse model uses the direct beam, the isotropic diffusion and the solar radiation diffusely reflected from the ground:



Figure 16: Map of Europe

$$I_T = I_b R_b + I_d \left(\frac{1 + \cos \beta}{2} \right) + I \rho_g \left(\frac{1 - \cos \beta}{2} \right) \quad (2.16)$$

where I is the horizontal radiation, I_b is the beam, I_d the diffusion on a horizontal surface and ρ_g the ground reflectance. R_b is defined as the ratio of the beam radiation on tilted surfaces to that on horizontal surfaces⁵. β is the angle between the horizontal and the module, taken equal to each city's latitude.

Weather data polynomials

Two second order polynomial expressions were determined, one for the temperature and one for the irradiation. For the solar radiation, regression analysis was made to irradiation data values higher than 100 Wh/m². Lower values of irradiation were giving an opposite curvature to the data line, which would lead to a higher order polynomial. This would make the calculations more complicated without adding any value to our results.

The temperature data were taken respective to the filtered irradiation data time period; e.g. if the irradiation values were higher than 100 Wh/m^2 between the time period of 11am to 4pm (Figure 17), the temperature values from the same time period were used to create the temperature polynomial. The polynomial functions replaced the ambient temperature term, T_a , and the irradiation in the solar fraction term, S , in equation (2.7). In this way the hourly variations of temperature and solar intensity is accounted in the model.

Daily energy outputs

Using the equation (2.5), the system's thermal gain is obtained. A system controller will take into account only the positive values of the thermal gain from the PV/T module (equ. (2.2) >0); there is no fluid circulation through the module if there is no thermal energy gain. The area is taken to be equal to the aperture PV cell's area, which is 1.2m^2 , while the heat loss coefficient was calculated through equations (2.8) and (2.9) adding the back loss coefficient. The variables in this relation are the heat removal factor, the solar intensity and the ambient temperature. The water

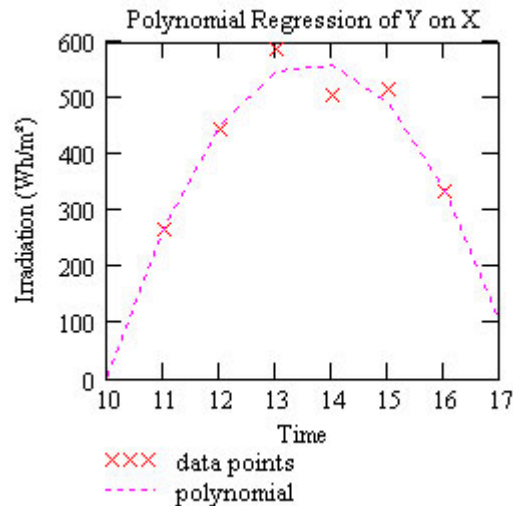


Figure 17: Irradiation data points and polynomial

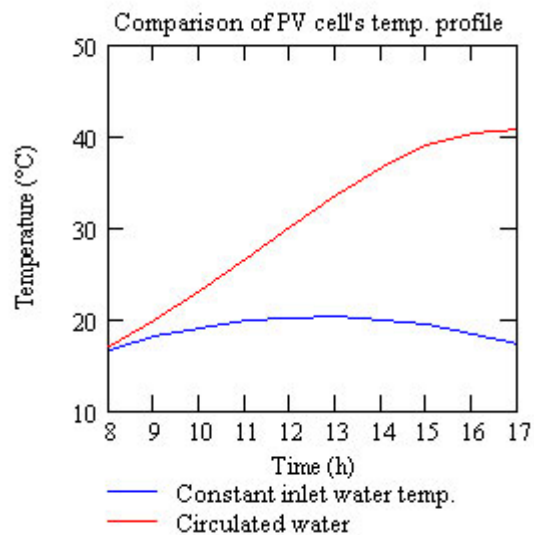


Figure 18: Comparison of PV cell's temperature profiles in two different module configurations during sunshine hours on a Greek summer day.

temperature at the storage tank can be found from equation (2.7). This represents the stored water temperature, T_w , and in the case that the water is circulated it also represents the inlet water temperature, T_i .

The system's inlet water temperature affects significantly the electrical energy output, Q_e . This can be noted from Figure 18, as the PV cell gets lower temperature values when the system is supplied with constant water temperature of 13°C. The lower temperature indicates the higher performance the photovoltaic conversion has when such a module configuration exists. The benefit in this particular example reaches at 1.16%. Similarly, equation (2.1), which is the electrical-energy-yield-relation, has variables, the solar intensity, the heat removal the thermal efficiency and the inlet water temperature (extended from equation (2.11)). The absorptance, a_{PV} , of the PV material was taken equal to 84%.

Relating the energy outputs with F_R

The relationships derived from the previous step give a linear

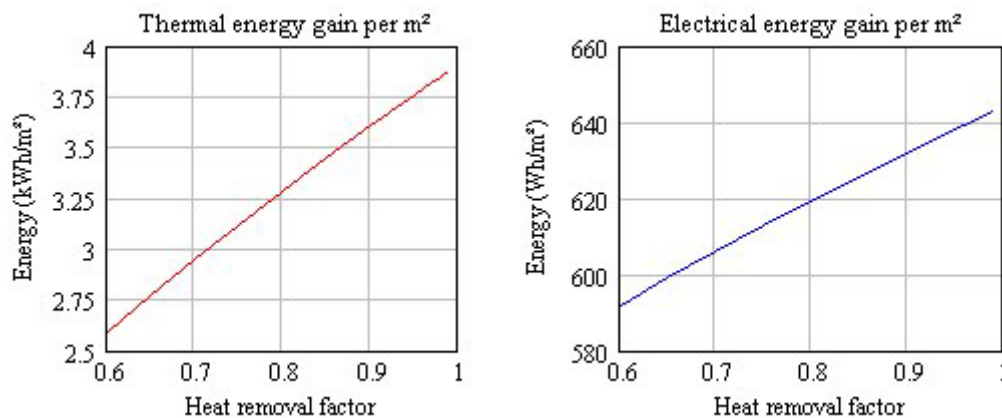


Figure 19: Energy gains for Brussels in a summer day.

relation between the energy gains and the heat removal factor, F_R (Figure 19). Applying a first order regression analysis we can have a linear relationship of the format $y=xa+b$, where y is the energy gain and x the heat removal factor. The slope, a , and the y -intercept, b , are uniquely derived from each weather file. As a result, by giving any value to the slope-factor x , that represent F_R , we can derive the daily energy yield for the particular city at the particular weather conditions.

Relating the flow rate to the heat removal factor

The next step is to relate the heat removal factor of different PV/T configurations to the flow rate. To achieve that, a steady state model was created using the equations mentioned in the beginning of this chapter. The process was created using MathCAD and to obtain the results it applies an iteration, as described by Duffy and Beckman⁵, adding though the photovoltaic effect. The iteration from the MathCAD file is illustrated on the next two pages:

Heat transfer coefficient for the wind

$$h_{\text{wind}} := \left[\max \left[5, \frac{8.6 \left(\frac{V_{\text{wind}} \cdot s}{m} \right)^{0.6}}{\left(\frac{L}{m} \right)^{0.4}} \right] \right]$$

Given (Start of the iteration solving block)

Glazing layer temperature

$$T_{\text{gl}} = T_{\text{PV}} - \frac{U_{\text{top}} \cdot (T_{\text{PV}} - T_{\text{a}})}{h_{\text{conv}} + \frac{\sigma \cdot (T_{\text{PV}} + T_{\text{gl}}) \cdot (T_{\text{PV}}^2 + T_{\text{gl}}^2)}{\frac{1}{\varepsilon_{\text{PV}}} + \frac{1}{\varepsilon_{\text{g}}} - 1}}$$

$$\text{Nu} = \left\{ \begin{array}{l} \beta' \leftarrow \frac{1}{T_{\text{air}}} \\ \text{Ra} \leftarrow \frac{g \cdot \beta' \cdot (T_{\text{PV}} - T_{\text{gl}}) \cdot L_{\text{sp}}^3}{\nu \cdot \alpha} \\ \text{Nu1a} \leftarrow \left[\sqrt[3]{\frac{\text{Ra} \cdot \cos(\beta)}{5830}} - 1 \right] \\ \text{Nu1} \leftarrow \left\{ \begin{array}{l} \text{Nu1a if Nu1a} > 0 \\ 0 \text{ otherwise} \end{array} \right. \\ \text{Nu2a} \leftarrow \left(1 - \frac{1708}{\text{Ra} \cdot \cos(\beta)} \right) \\ \text{Nu2} \leftarrow \left\{ \begin{array}{l} \text{Nu2a if Nu2a} > 0 \\ 0 \text{ otherwise} \end{array} \right. \\ 1 + 1.44 \cdot \left[1 - \frac{1708 \cdot (\sin(1.8 \cdot \beta))^{1.6}}{\text{Ra} \cdot \cos(\beta)} \right] \cdot \text{Nu2} + \text{Nu1} \end{array} \right.$$

$$h_{\text{conv}} = \frac{\text{Nu} \cdot k_{\text{air}}}{L_{\text{sp}}}$$

Sky temperature

$$T_{\text{sky}} := 0.05532 \cdot \left(\frac{T_{\text{a}}}{\text{K}} \right)^{1.5} \cdot \text{K}$$

Air temperature approximation between the glazing layer and the PV

$$T_{\text{air}} = \frac{T_{\text{PV}} + T_{\text{gl}}}{2}$$

Nusset number for estimating the convection coefficient between two parallel plates, the glazing layer and the PV.

Convection coefficient for the natural convection between the glazing area and the PV.

Top loss coefficient for one glazing layer (top) and for no glazing layer (bottom)

$$U_{top} = \left[\frac{1}{h_{conv} + \frac{\sigma \cdot (T_{PV} + T_{gl}) \cdot (T_{PV}^2 + T_{gl}^2)}{\frac{1}{\epsilon_{PV}} + \frac{1}{\epsilon_g} - 1}} + \frac{1}{h_{wind} \cdot \frac{watt}{m^2 \cdot K} + \sigma \cdot \epsilon_{PV} \cdot (T_{PV} + T_{sky}) \cdot (T_{PV}^2 + T_{sky}^2)} \right]^{-1} \text{ if } N = 1$$

$$\left[\frac{1}{\frac{k_{PV}}{\delta_{PV}}} + \frac{1}{h_{wind} \cdot \frac{watt}{m^2 \cdot K} + \sigma \cdot \epsilon_{PV} \cdot (T_{PV} + T_{sky}) \cdot (T_{PV}^2 + T_{sky}^2)} \right]^{-1} \text{ otherwise}$$

Overall heat loss coefficient

$$U_L = U_{top} + U_{back}$$

Heat removal factor (F' is the fin efficiency factor)

$$F_R = \frac{m_w \cdot C_p}{A_c \cdot U_L} \cdot \left(1 - \exp\left(\frac{-A_c \cdot U_L \cdot F'}{m_w \cdot C_p}\right) \right) \quad F' = \frac{1}{1 + \frac{U_L}{h_f}}$$

Thermal gain for the system

Solar fraction gained from the thermal system

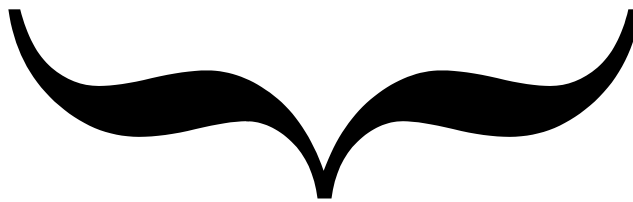
$$Q_T = A_c \cdot F_R \cdot [S - U_L \cdot (T_i - T_a)] \quad S = \left(\tau\alpha - \eta_{PV} \cdot \frac{A_{pv}}{A_c} \right) \cdot I$$

Module temperature

Thermal system efficiency

Electrical system efficiency

$$T_{PV} = T_i + \frac{1 - F_R}{F_R \cdot U_L} \cdot \eta_T \cdot I \quad \eta_T = \frac{Q_T}{A_c \cdot I} \quad \eta_{PV} = \eta_{ref} - \mu \cdot (T_{PV} - T_{ref})$$



Simplification made to ease the iteration

$$T_{PV} = \frac{[(-\tau\alpha \cdot F_R + \tau\alpha) \cdot I + (T_i - T_a) \cdot U_L \cdot F_R + T_a \cdot U_L] \cdot A_c + [(\eta_{ref} + \mu \cdot T_{ref}) \cdot A_{pv} \cdot F_R + (-\eta_{ref} - \mu \cdot T_{ref}) \cdot A_{pv}] \cdot I}{[(\mu \cdot A_{pv} \cdot F_R - \mu \cdot A_{pv}) \cdot I + U_L \cdot A_c]}$$

Find($U_{top}, U_L, T_{PV}, F_R, T_{gl}, T_{air}, Nu, h_{conv}, F'$)

(End of solve block)

As for the PV module's characteristics a commercial monocrystalline cell was used with $I_{mp}=4.52A$, $V_{mp}=35.4V$, covering an area equal to $1.2m^2$ and having 13% efficiency under standard test conditions(STC). For the wall-to-wall system, the square tubes that cover the back of the module are perceived to have very thin walls with low thermal resistance and were taken with a hydraulic diameter of 10 mm. The fluid inlet temperature was set for all cases at $13^{\circ}C$ and the modules orientation at 45° to the horizon. The rest of the material properties and the constraints used in the above process are reported in the appendix. As for the climatic conditions, the average values of each analyzed day were used. This can be thought of as a good approximation, since the daily optimum conditions are required and the hourly fluctuation of temperature and irradiation does not matter.

The above model does not take into account the temperature variation on the PV module as Bergene and Lovvik⁴ do with their model. Nevertheless, J.P. Berry¹⁸ reports in his work that a gradient temperature of $15^{\circ}C$ from $60^{\circ}C$ has very little influence on the power provided by a photovoltaic module, meaning that as long as the temperature difference between any PV cell is kept up to $15^{\circ}C$ the electricity production calculations are not penalized.

Using the VisSim¹⁷ simulation package the model was fed with different flow rate values. The flow rate interval in the simulation program was set to $0.002kg/s$ starting from 0 and ending to $0.1kg/s$. It has been identified that this is the most

significant area for concentrating the results. Two setups were used, a glazed and an unglazed wall-to-wall. The sheet-and-tube setup, due to a

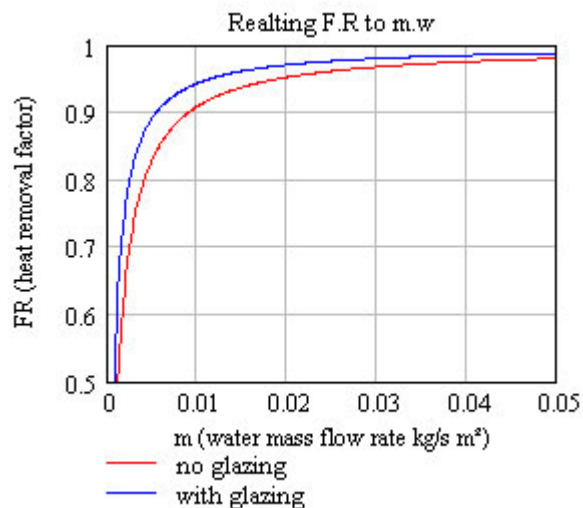


Figure 20: Graph relating the mass flow rate and the heat removal factor in a Greek summer day

smaller fin efficiency factor, F' , is less efficient than the wall-to-wall. The serpentine setup tends to approach the sheet-and-tube characteristics, as mentioned earlier, and is more beneficial when used with a stratified tank and with very low flow rates. Some errors were noticed in the simulations; most probably because of the convergence tolerance used in the MathCAD file (was set to 0.0001) in combination with the iteration process. The errors were smoothed in the analysis by a median smoothing function that is included in MathCAD.

The result of the above process is a direct relationship between the mass flow rate, \dot{m} , and the heat removal factor F_R as illustrated in Figure 20.

System's surcharge due to water pumping

The greater the flow rate the higher the heat removal factor is, which derives higher energy gain values. Assuming that the system does not use natural water circulation, the water is circulated by the use of a pump which is powered from the system's photovoltaic module. The higher the flow rate the higher the energy required for the pump to drive the system, while when the flow rate reaches the critical value, where the flow becomes turbulent, the pump input increases rapidly. Turbulent flow increases the heat removal factor as well (see Figure 14).

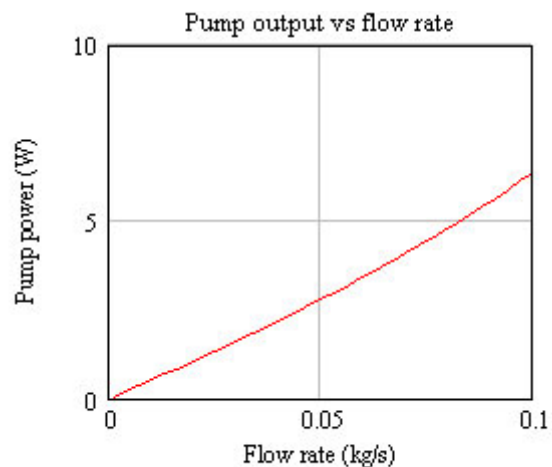


Figure 21: Pump's power requirements

Turbulence though occurs at flow rates, where the pumping requirements are very large and outreach the thermal benefit we get from the increased heat removal factor¹⁵. Based on the extended Bernoulli energy equation for incompressible steady flow, a pump's reaction is examined by simulating different flow rates. A hydraulic diameter of 10 mm is taken while the pump's efficiency, η_{pump} , is taken to be equal to 18.6% (this value was taken from the WILO ST 25-4 circulation pump

characteristics¹⁹), the head is one meter and the pipe smooth;

$$P = m_w \left(g \cdot head + fr \cdot \frac{L}{D} \cdot \frac{v_f^2}{2} \right) \cdot \frac{sunshine_hours}{\eta_{pump}} \quad (2.17)$$

In this equation g is the gravitational force, fr is the friction factor, L is the pipes length which was taken equal to the modules width, D is the hydraulic diameter, v_f is the fluid velocity and "sunshine_hours" represents the daily time period that the pump is operating; this is just the hours of the day that the irradiation is higher than 100 Wh/m². For this particular hydraulic diameter turbulence is formed at 0.01kg/s.

Energy yield and application of economic tools

The energy yield is derived by an algebraic aggregation of the energy sources. A total energy yield can be obtained by adding the thermal with the electrical energy gained, and subtracting the energy used by the pump:

$$total_E = Q_u + Q_e - P \quad (2.18)$$

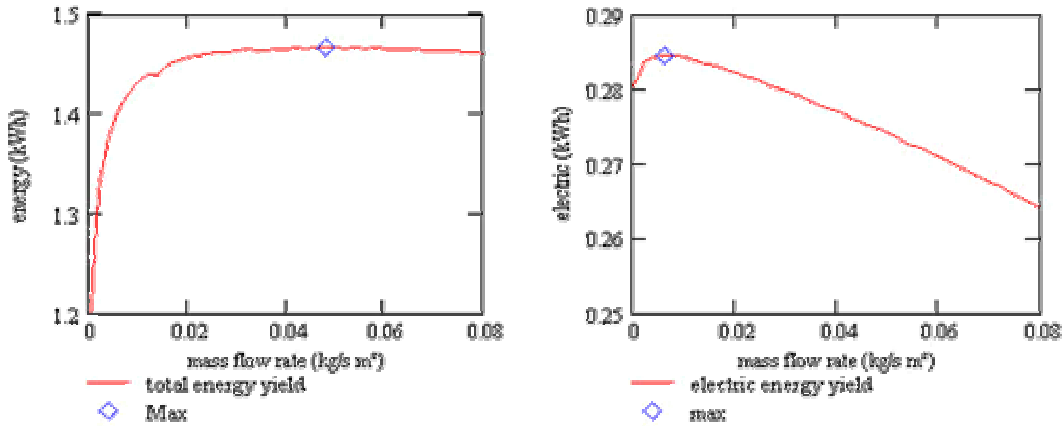


Figure 22: Energy yields for a winter day in Brussels

An electrical energy yield can also be obtained as the residual from subtracting the pump's consumed energy from the PV's generated energy:

$$electic_E = Q_e - P \quad (2.19)$$

These expressions give a parabolic relationship between the flow rate and the energy yield. The optimum flow rate is at the maximum point of this parabola. Figure 22 illustrates such a representation for Brussels where the optimum flow rate to the total energy is at 0.048 kg/m²s and

gives a daily energy yield, electrical and thermal, of 1.467kWh. For the electrical system the optimum flow rate conditions exist at 0.007 kg/m²s. This flow rate would produce 284Wh during the day from this single module.

Thermal and electrical energy do not have the same price value. In fact electricity is more expensive than thermal energy and the algebraic aggregation should be weighted accordingly to derive proper results. By

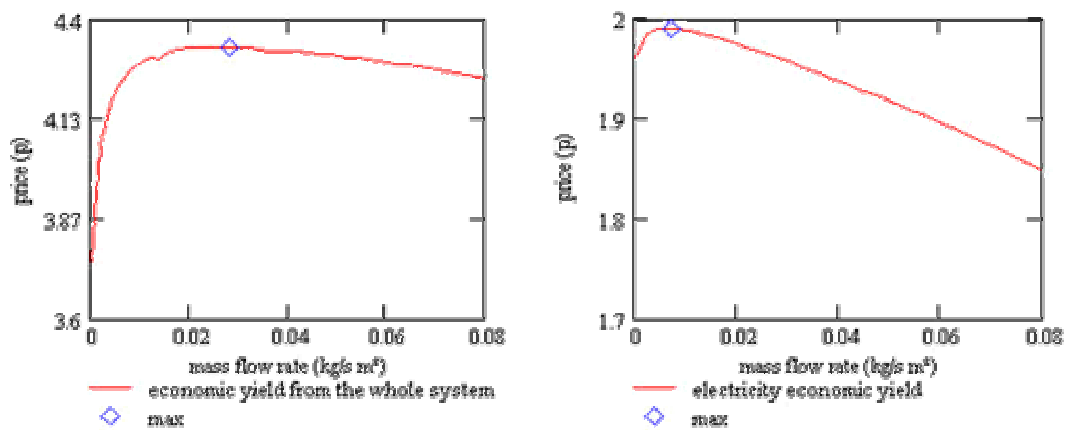


Figure 23: Economic yields for a winter day in Brussels

applying typical energy price values to the previous relationships the maximum energy value generated by the system can be acquired. That maximum point resolves the optimum flow conditions. The energy values used were 7p/kWh for electricity and 2p/kWh for thermal energy. In Figure 23 is illustrated that the optimum conditions for the electrical system remained the same. The analysis of the total system on the other hand, shows a lower optimum flow rate, 0.028kg/m²s. This is the result of the price weight that was applied to the factors of the total energy yield equation.

Conclusions

In this chapter a method to identify the optimum flow rate conditions was formed based on existed, validated relationships. This method is translated into a mathematical model, built in MathCAD, and it will be used with three different climate files representing different European latitudes, to see if the optimum flow rate varies with it.

-
- ¹² Kleinbach, E., Beckman, W., Klein S., "Performance study of one-dimensional models for stratified thermal storage tanks" 1993, Solar Energy, Vol. 50 No. 2, pp. 155-166
- ¹³ Saidov M.S., Abdul'nabi Z. M., Bilyalov R.R. and Saidov A. S. "Temperature characteristics of silicon solar cells" Appl. Solar Energy Vol. 31, 1995
- ¹⁴ Zhang H. and Lavan, Z "Thermal performance of a serpentine absorber plate" Solar energy Vol. 34, 1985
- ¹⁵ Dayan M., Klein S., Beckman W. "Analysis of serpentine collectors in low flow systems", American Solar Energy Society, 1998
- ¹⁶ Mathsoft Inc, <http://www.mathsoft.com>
- ¹⁷ Visual Simulations Inc, <http://www.vissim.com>
- ¹⁸ J. P. Berry "Simulation ELDO et SPICE" Laboratoire LAAS, Toulouse, 1997
- ¹⁹ The Online Pump Magazine. <http://www.impeller.net>

CHAPTER 3

Validation

The decision to build a simulation process similar to the simple thermal system simulation was made due to the fact that these processes are already validated throughout the past years and, similarly, should be valid for a PV/T system. Indeed, the studies of Krauter *et al.* (1999)⁹ and Sandnes *et al.* (2001)⁶ serve as evidence to prove that. The validation of the above mentioned differential equation (2.7), has been performed by Sandnes *et. al* (2001)⁶ with the only difference that they have used an additional heat input from the circulation pump. Applying their values for

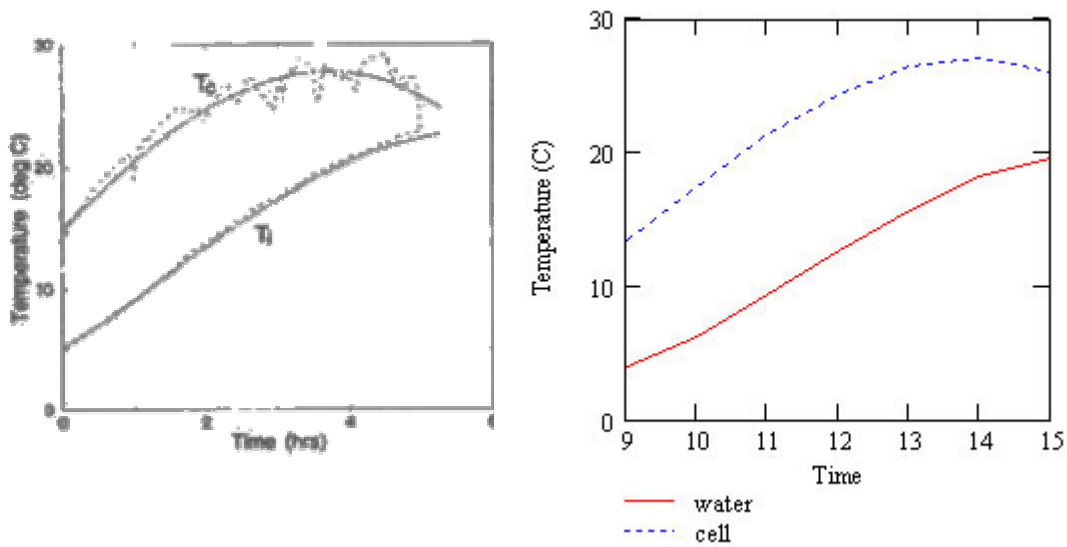


Figure 24: Simulation comparison results with Sandnes *et al.*

F_{RTa} and F_{RU_L} and two polynomials representing Oslo's solar radiation and ambient temperature for a clear day in March, a temperature profile for the PV/T plate and the stored water is produced. The temperature profiles are similar to the ones produced by Sandnes (Figure 24). This proves that if the model is based on these assumptions, the results derived for the PV/T energy outputs should be valid. Note that the slightly lower temperature that was obtained should be indeed because of the extra heat input from the pump (an additional thermal input value, $+L$, in equ. (2.7)). This additional input is not used in this study.

CHAPTER 4

Simulation and analysis

System configuration analysis

Two different system configurations were simulated in a circulation system (Figure 11a). The first PV/Thermal arrangement did not have an extra glazing layer (Figure 25a) and the second one had an extra glazing layer 25mm above the PV cells (Figure 25b). Moreover, the heat recovering medium used was water and the system had a storage capacity of 150 litters, which is assumed equal to the daily needs of a three-person family. Both system configurations were examined on the basis of how their performance alters with wind speed, so for each climate file two simulations had run; one with no wind and one with wind speed of 5m/s. The constant inlet water temperature setup (Figure 11b), was not simulated because the pump's head and work, depends on the tap water pressure, and storage varies with demand. This actually could be a study in itself. The results are categorized per latitude and per season to visualize the performance variations. The values on the graphs indicate the optimum flow rate in kg/m²s. The y-axis indicates the value someone would pay to acquire this energy from the market; in other words the higher the value is the more economically efficient becomes.

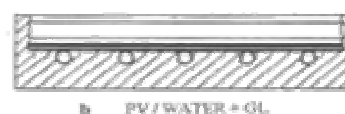
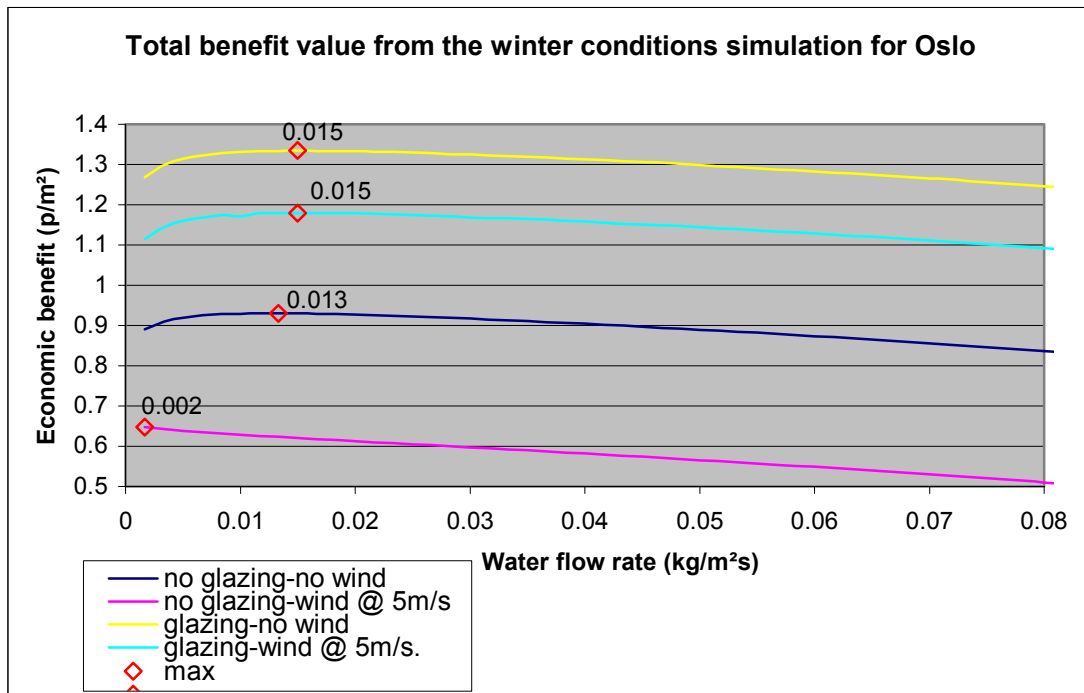


Figure 25: PV/T configurations

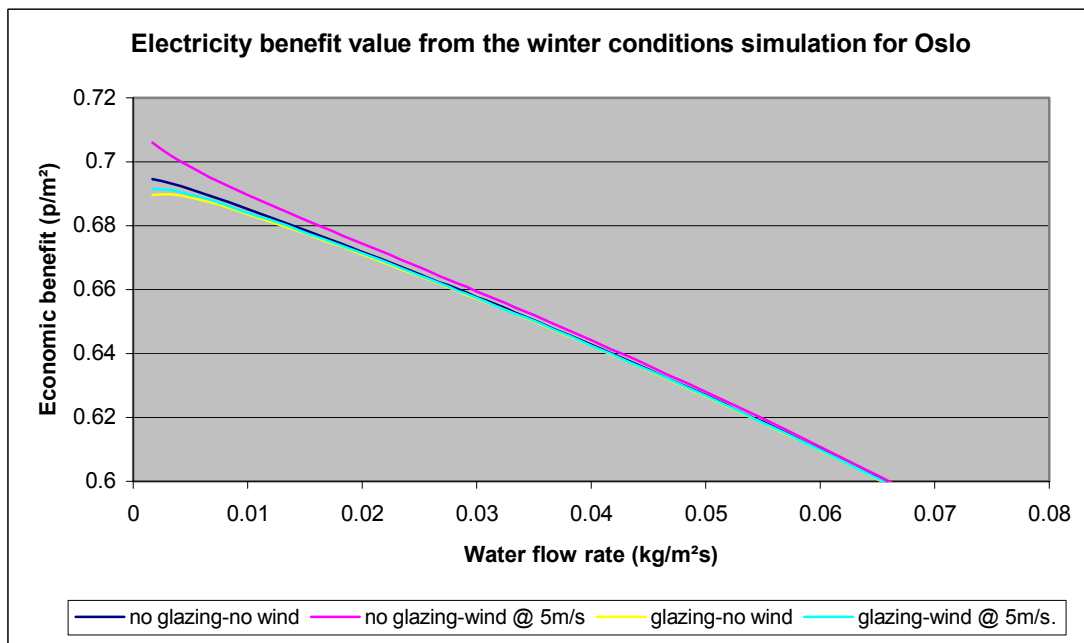
High latitude results

European high latitude areas are characterized from their cold weather conditions; very cold winter with low irradiation and limited sunshine hours, and mild summers with comfortable temperatures and long hours of sunshine. The winter weather profile for Oslo had an average ambient temperature of -5°C and 3 hours of sunlight with average irradiation equal to 229 Wh/m². The summer weather profile had average ambient temperature of 20.3°C and 9 hours of sunlight (with irradiation higher than 100Wh/m²). The average irradiation was 593

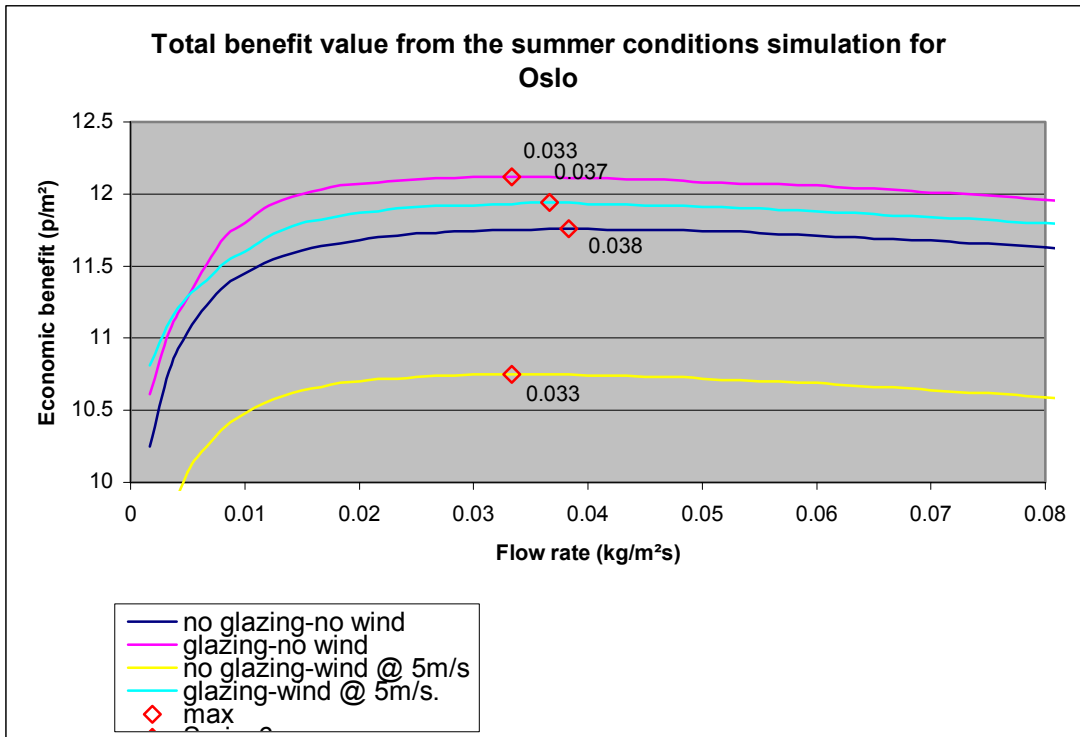
Wh/m² and for the winter simulations the initial water temperature was set to 7°C (instead of 13°C) because of the very low ambient temperatures.



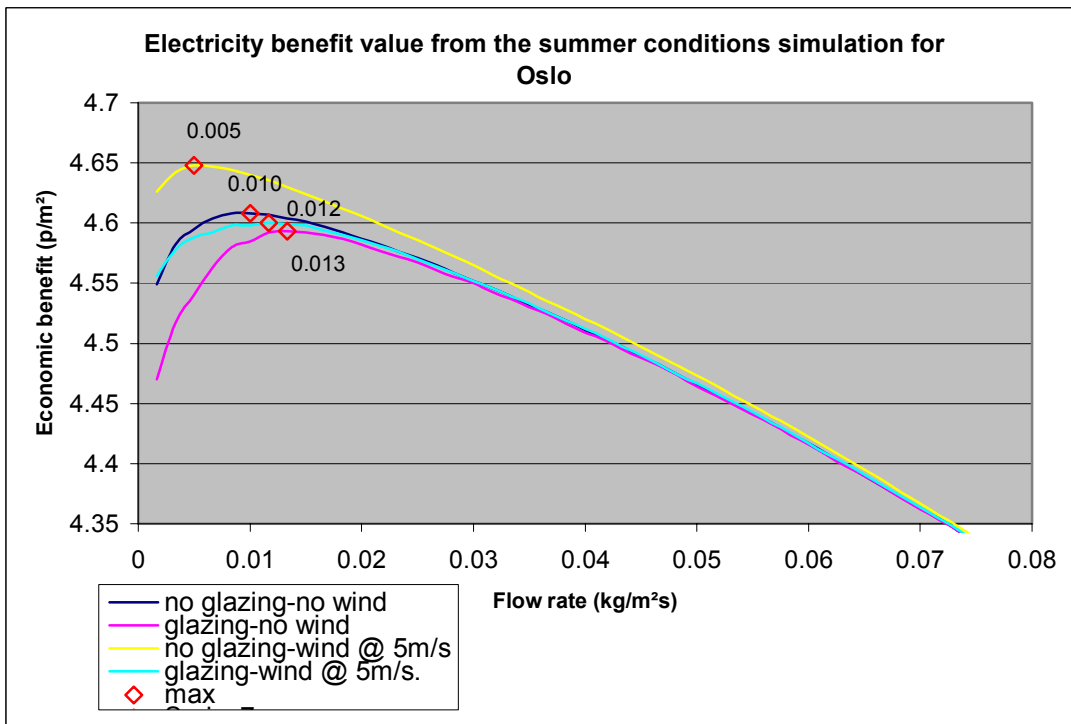
Graph 1



Graph 2



Graph 3



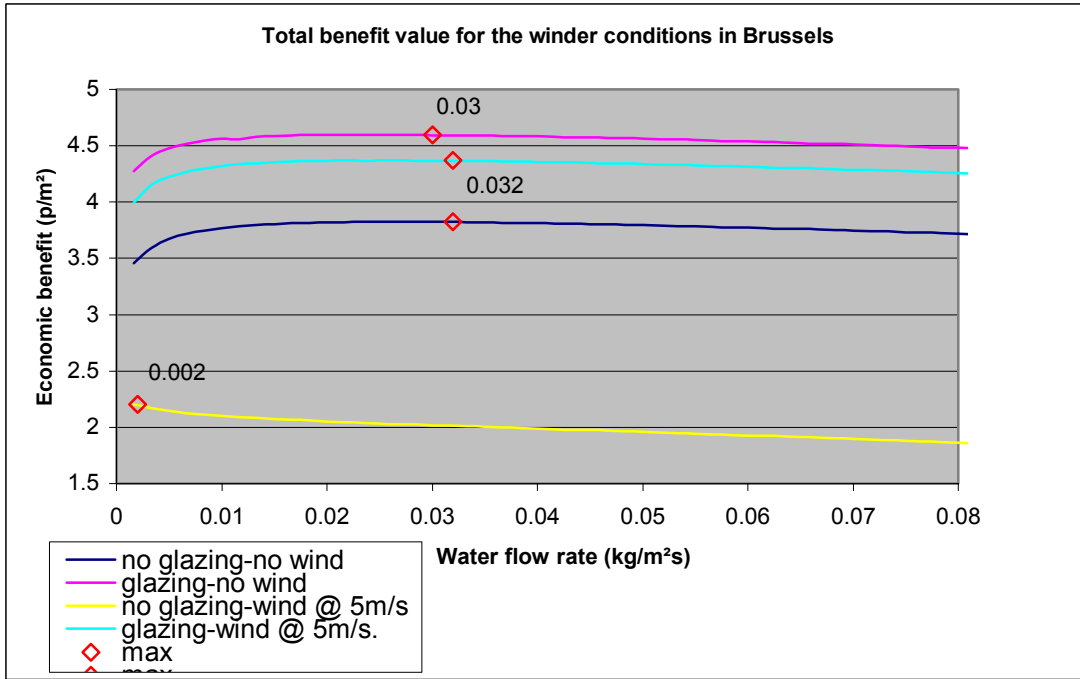
Graph 4

In this first set of simulations, the results for the two different configurations show that the extra glazing layer benefits the system to its total energy yield. For a flow rate of $0.015\text{kg/m}^2\text{s}$, in the winter simulation, the system generates energy equal to 0.4 pence/m^2 more than the unglazed system. For the summer simulation the optimum flow rate is at $0.033\text{kg/m}^2\text{s}$ for the glazed system without any wind effect.

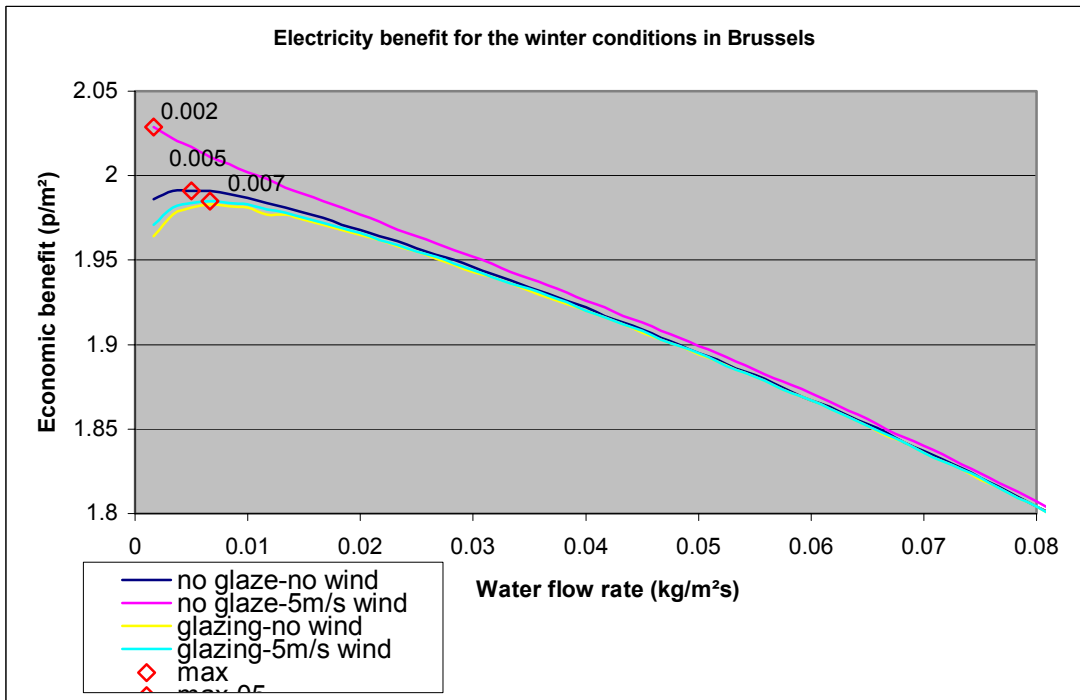
On the contrary, the unglazed configuration has better results for the plain electric system. Particularly, along with the wind effect, the optimum flow rate for the summer day simulation is $0.005\text{kg/m}^2\text{s}$. At these conditions the module generates electricity equal to 4.64 pence/m^2 or 0.66kWh/m^2 . In addition, we note that, due to the lower temperature levels, the electrical energy generation in the winter day simulation, has greater contribution to the total system, than in the summer day simulation.

Central latitude results

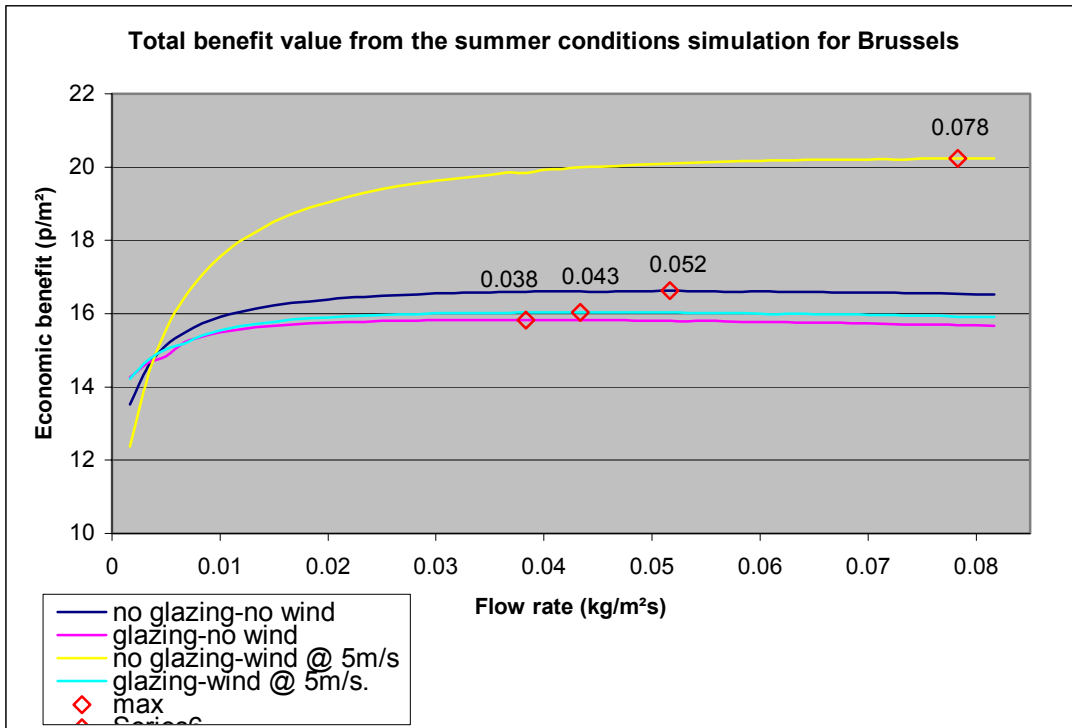
In the central European area the climate is characterized by mild conditions; warm summer and cold winter. Depending on the terrain and the proximity to the sea these attributes can fluctuate but never reaching extreme conditions. The Brussels weather file for the simulated winter day had an average ambient temperature of 4.4°C , 5 hours of sunshine and average irradiation of 442 Wh/m^2 . The relevant file for the summer simulation had an average ambient temperature of 25.6°C , 10 hours of sunshine and average irradiation of 605 Wh/m^2 .



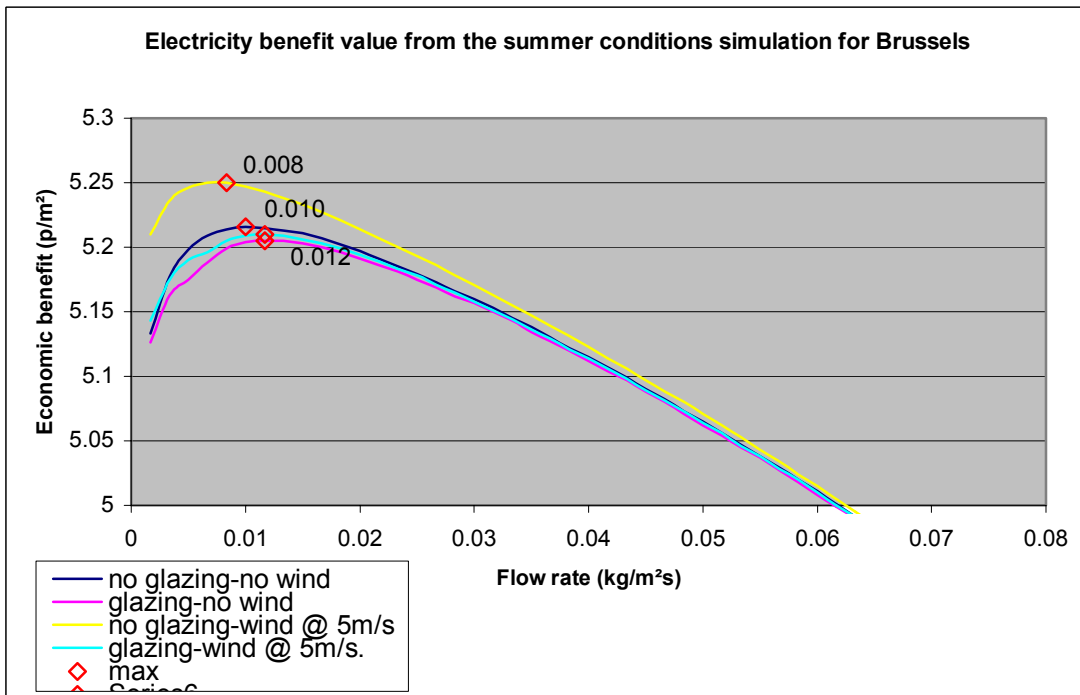
Graph 5



Graph 6



Graph 7



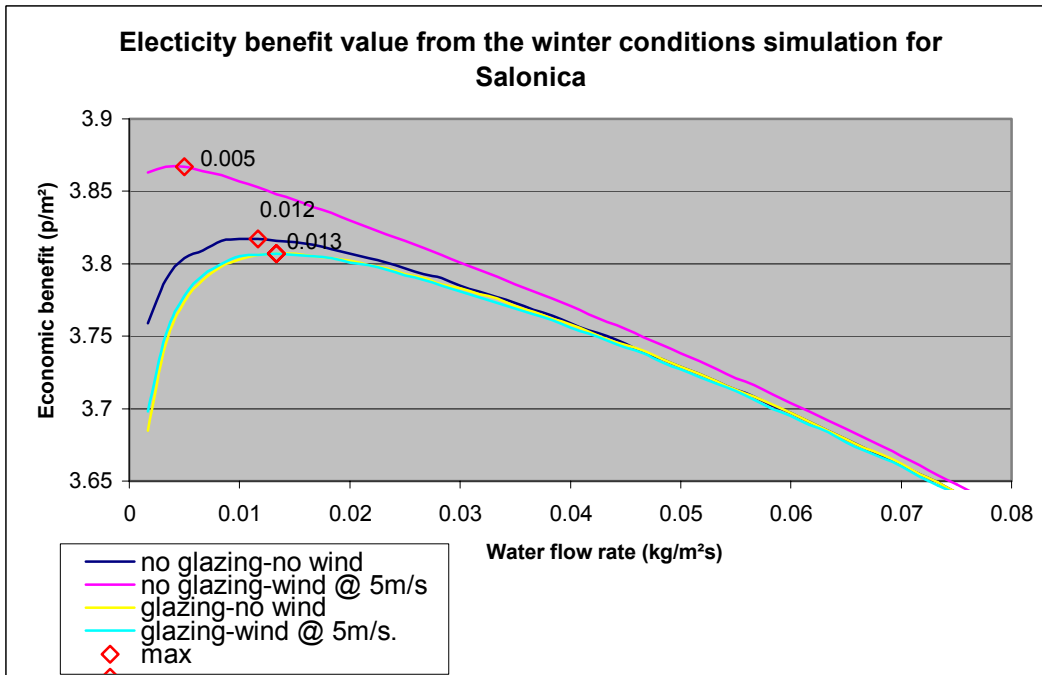
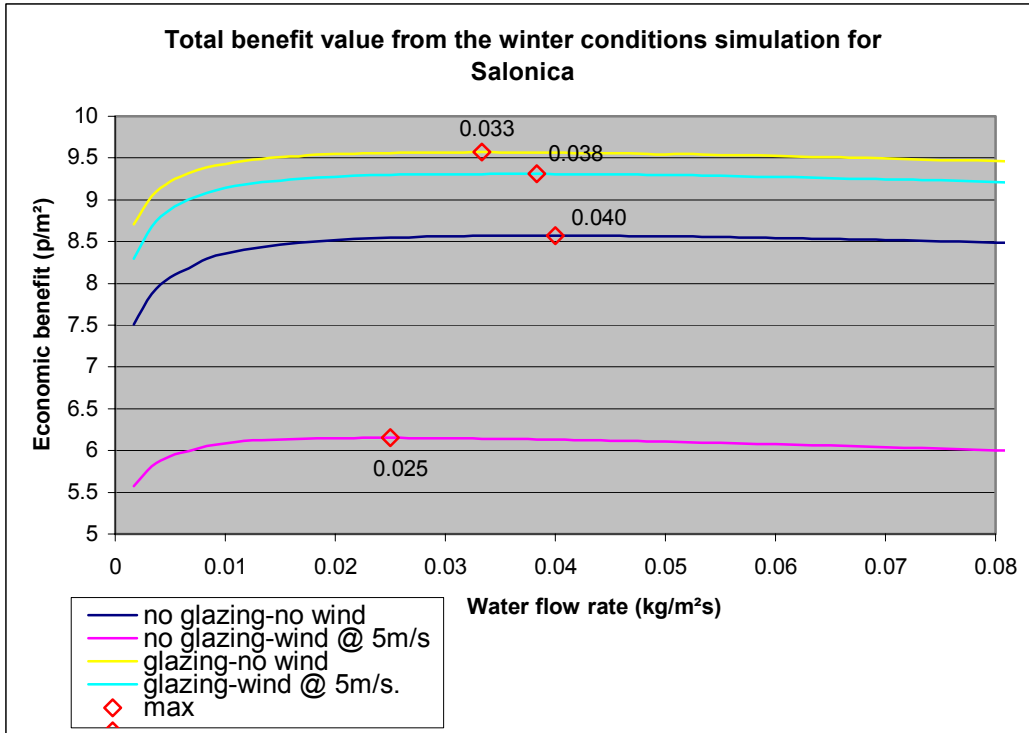
Graph 8

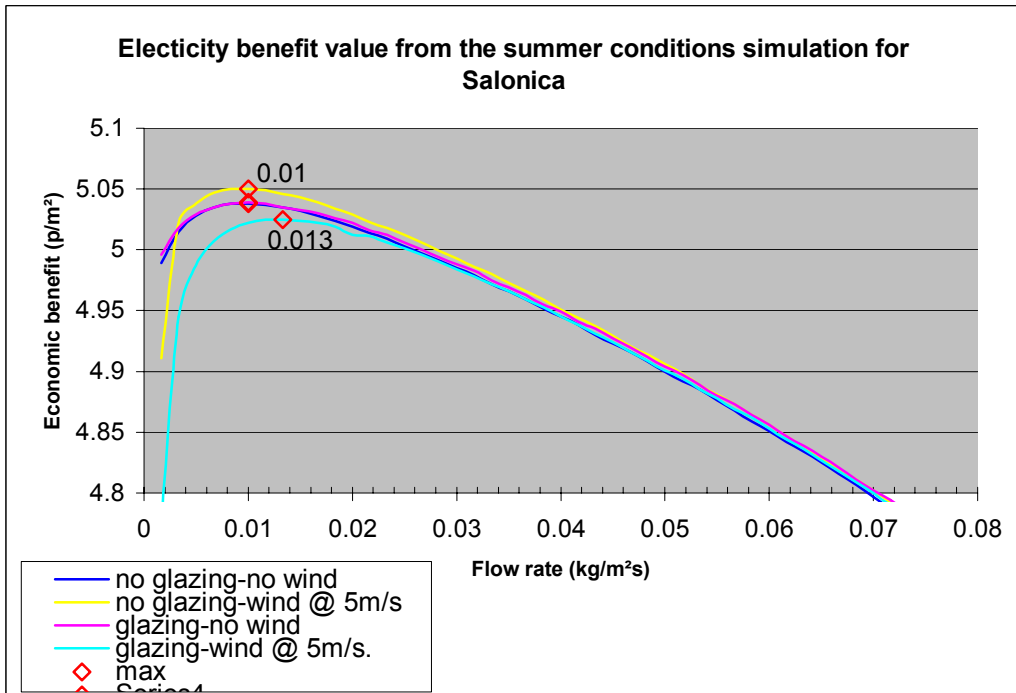
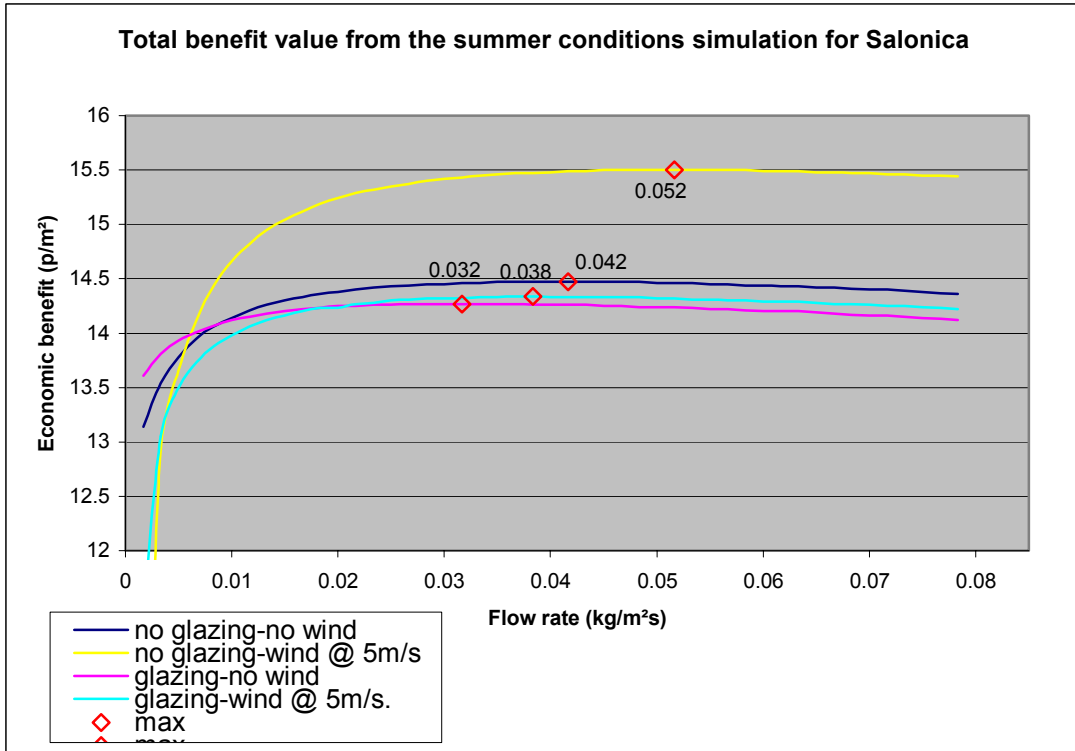
The simulations performed for the central latitude, show that the results for the winter day simulation are similar to those of the high latitude. The best configuration is the glazed one, producing a total energy yield equal to the price of 4.6pence/m² when the flow rate is equal to 0.03kg/m²s (for windless conditions).

On the contrary, the summer simulations show as the best configuration, for both total and electrical energy generation, the unglazed system. Particularly, analysing the system's total energy yield, the maximum generation value is equal to 20.2pence/m² at 0.078 kg/m²s for the unglazed configuration at windy conditions. This sounds unusual and most probably occurs because of the fact that electricity gets a higher grade when applying the economic scales, 0.7p/kWh instead of 0.2p/kWh that thermal energy gets. Moreover, the unglazed configuration benefits the photovoltaic conversion which seems to have a large contribution to the total economic benefit value. The electric system analysis for the summer simulation, gave an optimum flow rate of 0.008kg/m²s for the unglazed configuration at windy conditions. At that flow rate the system generates 0.75kWh/m² at the simulation day.

Low latitude results

The Mediterranean climate is the prominent feature in this latitude area; high temperatures throughout the year, with extremely hot conditions during the summer. These characteristics do not promote the photovoltaic generation, since the PV cells can reach temperatures higher than 80°C in some cases. The climate file used for the winter simulation of the Greek city had an average ambient temperature of 9.8°C, average irradiation of 709 Wh/m² and 6 hours of irradiation higher than 100Wh/m². The summer climate file had an average ambient temperature of 29°C, irradiation of 650Wh/m² and 9 hours of accountable sunshine.

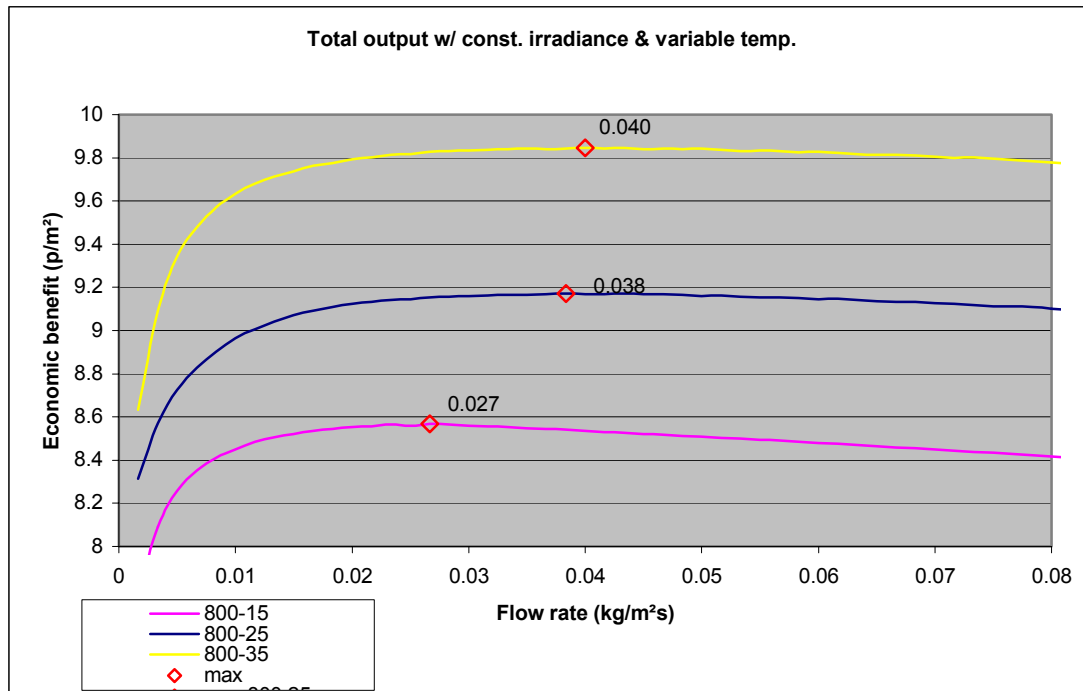




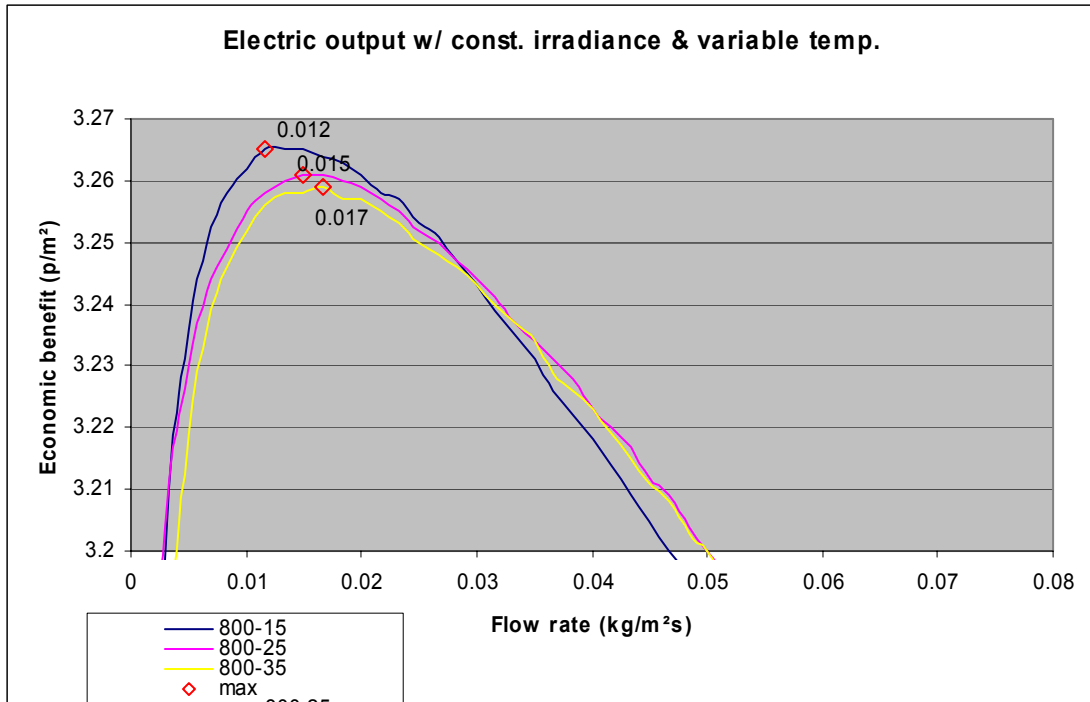
The simulations performed with the climate file of Thessaloniki gave results similar to the Brussels simulation ones. The differences are concentrated to the higher economic benefit values Thessaloniki gets during the winter, while during the summer these values are lower. The configuration that gets the bigger advantage is, again, the unglazed setup.

Parametric analysis

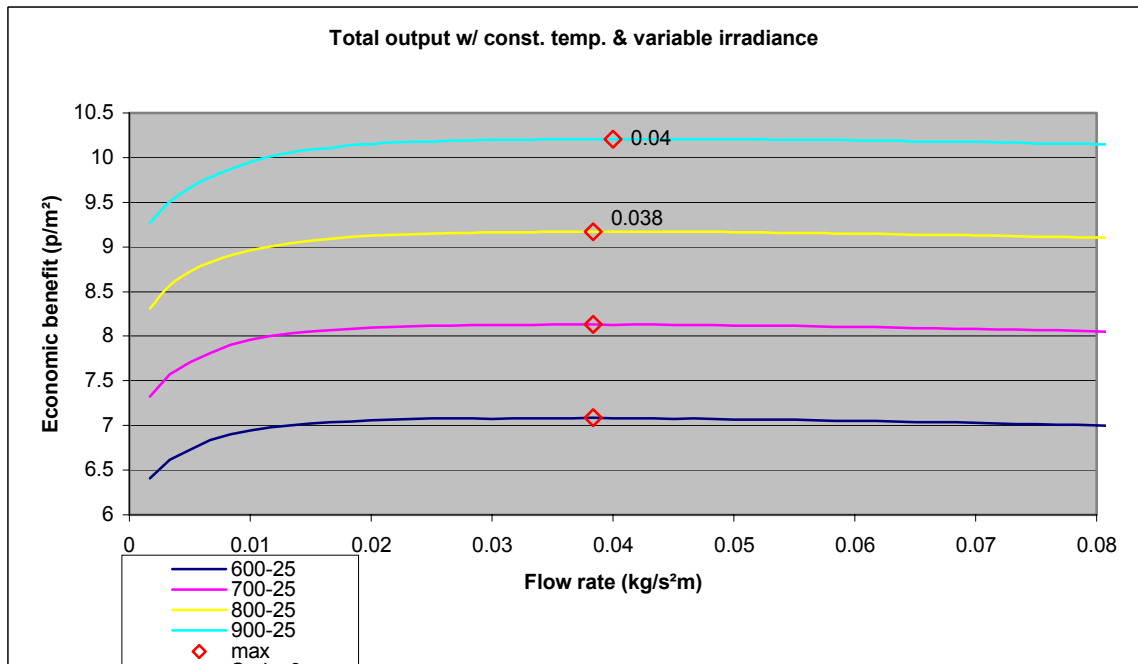
A set of simulations constructed with set irradiation and ambient temperature, independent from any climate. This parametric analysis is important in order to understand and reason the model's responses. In the first set of these simulations the irradiation was kept constant at 800Wh/m² (as this can represent a good solar intensity value for proper thermal and electrical generation) while the ambient temperature got values of 15°C, 25°C and 35°C. In the second simulation the temperature was kept constant at 25°C and the irradiation variable got values of 600Wh/m², 700Wh/m², 800Wh/m² and 900Wh/m². In both cases the wind variable was set to zero and the glazed configuration was used.



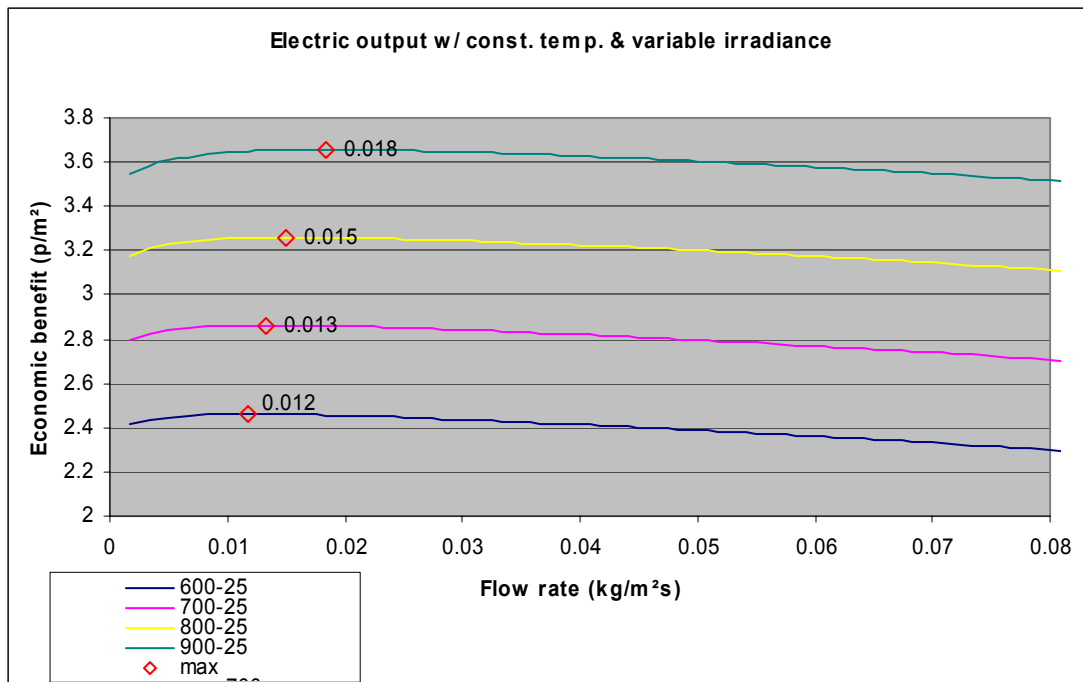
Graph 13



Graph 14



Graph 15



Graph 16

In this set of simulations an attempt was made to identify how the optimum flow rate changes with different irradiation and temperature levels. A general observation to the graphs shows that there is a shift to a bit higher flow rate as irradiation or temperature increases.

This does not occur to the energy gains though; as ambient temperature increases the photovoltaic generation decreases, though there is a larger contribution from the thermal part of the module. This is illustrated in Graph 13 and Graph 14. Starting from the second case (Graph 14) the electric generation diminishes as the ambient temperature rises, while there is an increase to the optimum flow rate. On the contrary, Graph 13 shows that as the ambient temperature increases, the optimum flow rate increases along with the module's total energy generation, showing that the thermal part is gaining an advantage and achieves a larger contribution to the system's outcome.

For the variable irradiation simulations, it is noted (Graph 15 and Graph 16) that as the irradiation levels increase the flow rate increases accordingly, particularly when analyzing just the electric system. The

irradiation level variation seems to affect more the thermal generation than the temperature variation does. This can be concluded by comparing the difference of economic benefit in Graph 13 and Graph 15; increasing the temperature by 10°C a benefit of 0.7p/m² at the optimum flow rate conditions is reached, while increasing the irradiation by 100Wh/m² a gain of 1p/m² is achieved. Note that the optimum flow rate is shifted to the same level in both cases.

Conclusions

Using the mathematical model discussed in the previous chapter, three simulation sets were performed using climate files from different representative European cities. The scope of the simulations is to identify how the optimum flow rate conditions, vary with latitude. Results show that in general, the warmer the climate the higher the flow rate. When the temperature levels reach a large value, the electricity generation decreases and reduces the available power to drive the water circulation pump, causing the optimum flow rate level to decrease accordingly. The discussion of these results follows in the next chapter.

CHAPTER 5

Discussion of Results and Conclusions

Discussion

The photovoltaic thermal module is formed by two main parts; the thermal collector and the PV cells. The thermal collector is benefit by high temperatures and low heat losses while the PV cell is gaining an advantage when temperatures are low and the heat loss coefficient gets a large value. Either parts need of course high levels of solar irradiation. By combining these two parts to build a single module, we either have to compromise with the benefit of one part to the benefit of the other, or find a total optimum condition. By using economic tools the produced energy can be rated and the optimum flow rate would correspond to both, the thermal and the electrical energy daily gains.

The sun paths and the daily irradiation time shown in Figure 26

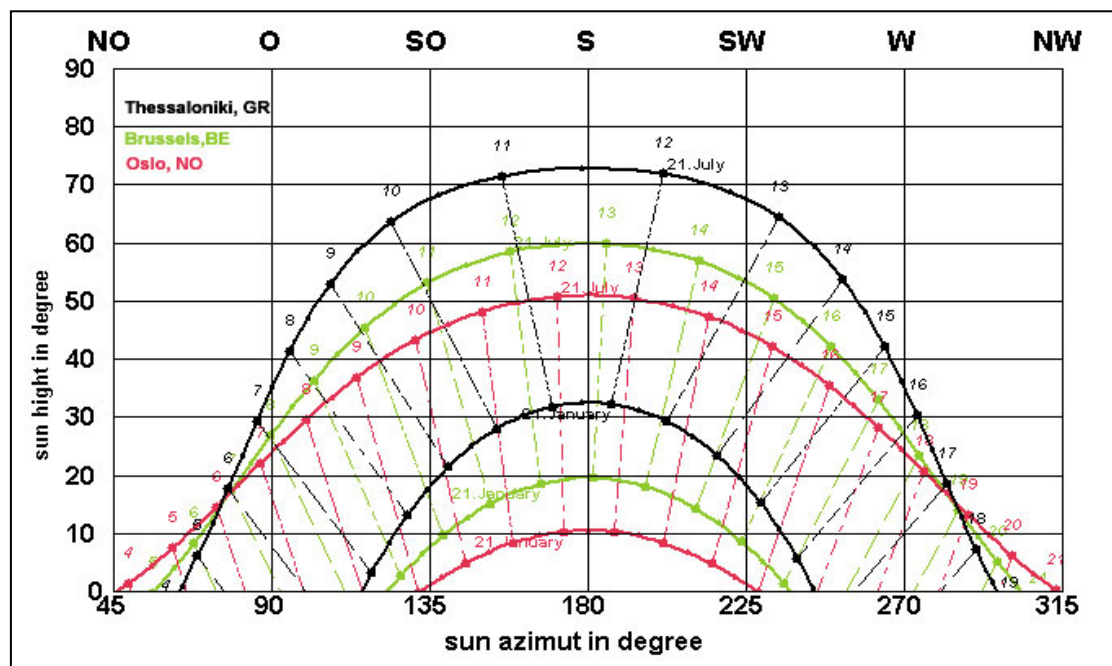


Figure 26: Sun positioning plot at the three examined city latitudes

identify the different properties each of the three examined latitudes has. The low latitude city of Thessaloniki, having the sun higher than the other two cases, gets a larger amount of irradiation due to the fact that the sun beam crosses a smaller quantity of atmospheric mass causing less

diffusion (Figure 27). This is relevant to the air mass, m_{air} , which is part of the R_b parameter in equation (2.16) and is defined as the ratio of the mass of atmosphere through which beam radiation passes to the mass it would pass through if the sun was directly overhead.[2]

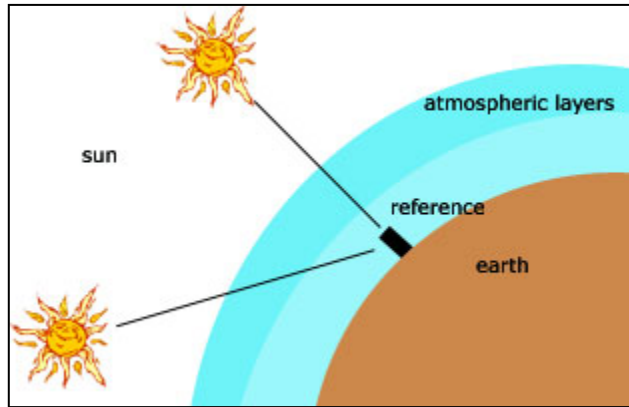


Figure 27: Sun beam magnitude through the atmosphere to a reference object

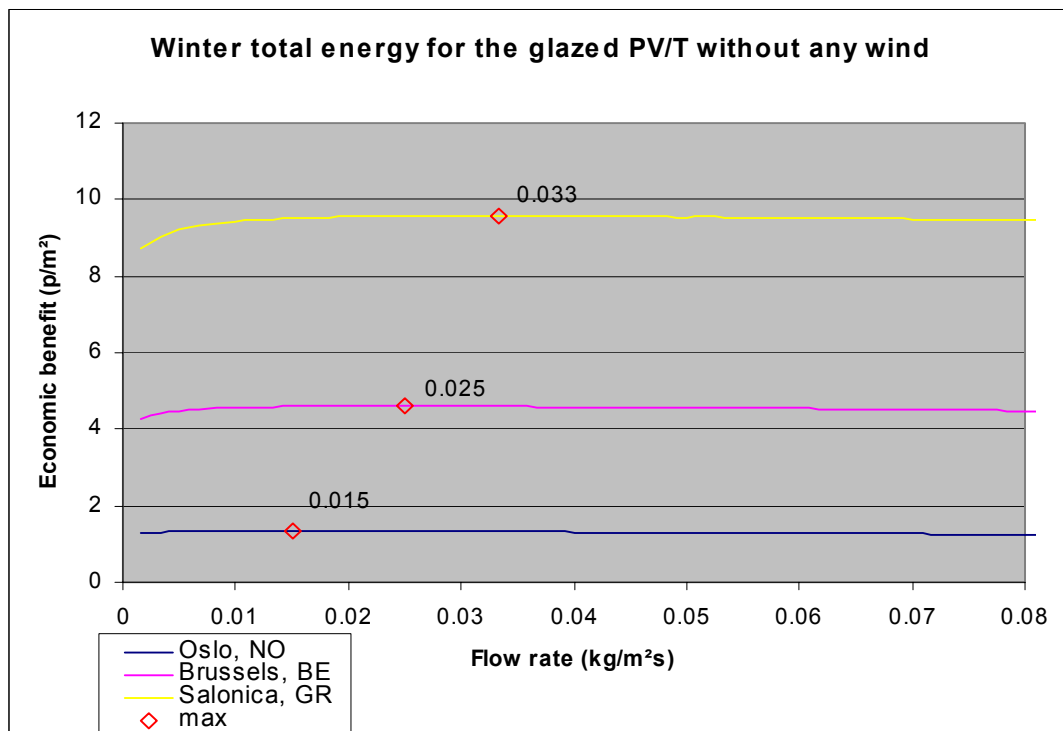
Consequently, despite of the fact that the higher latitudes have longer summer days, the average daily irradiation is higher in lower latitudes, causing higher ambient and module temperatures.

This temperature rise deprives the electric system from generating energy, and someone would expect to have a higher flow rate through the module in the low latitude case study than in the high latitude one. This would decrease the module's temperature and increase its electricity energy generation efficiency. A higher flow rate though, would require more electricity to drive the water pump, and that has an effect on the system's energy yield. The pump's energy requirements is derived from the second order equation (2.17), and the increase of the photovoltaic conversion efficiency is related to the linear equation (2.13). At the point that the rate of energy required to drive the pump becomes equal to the rate of generated energy, the optimum system condition is reached. For the total energy analysis, there is an extra energy input that is related to the thermal efficiency, equation (2.12). To derive the optimum flow rate for the total-energy-yield, the rate of this equation is added to the previous argument. This optimum conditions obtained here are different from the thermodynamic optimum conditions.

The thermodynamic optimum conditions differ in the sense that the energy required to drive the pump does not account; the higher the flow rate is, the higher the heat removal factor becomes (Figure 20). As a

result, using a high flow rate, due to the water's thermal diffusivity, the tank's water temperature increases slower while the PV cells keep a low temperature as long as the inlet, storage tank, temperature is low. Depending on the demand along with the tank's size, temperature variation and gradient, the flow rate can be adjusted according to the primary module's use at each instance. A lower flow rate will increase the thermal energy gain, particularly in a stratified tank, while a high flow rate will decrease the module's temperature and increase its electric conversion ability. In other words, two thermodynamic optimum conditions exist, one for the thermal and one for the electrical system, and depending on the generation type necessity, the more appropriate one should be chosen. To determine the flow rate values necessary for each instance, either the heat flux equations used by Krauter *et al.*⁹, or those derived by Bergene and Lovvik⁴ can be incorporated to the control system that manages the flow rate.

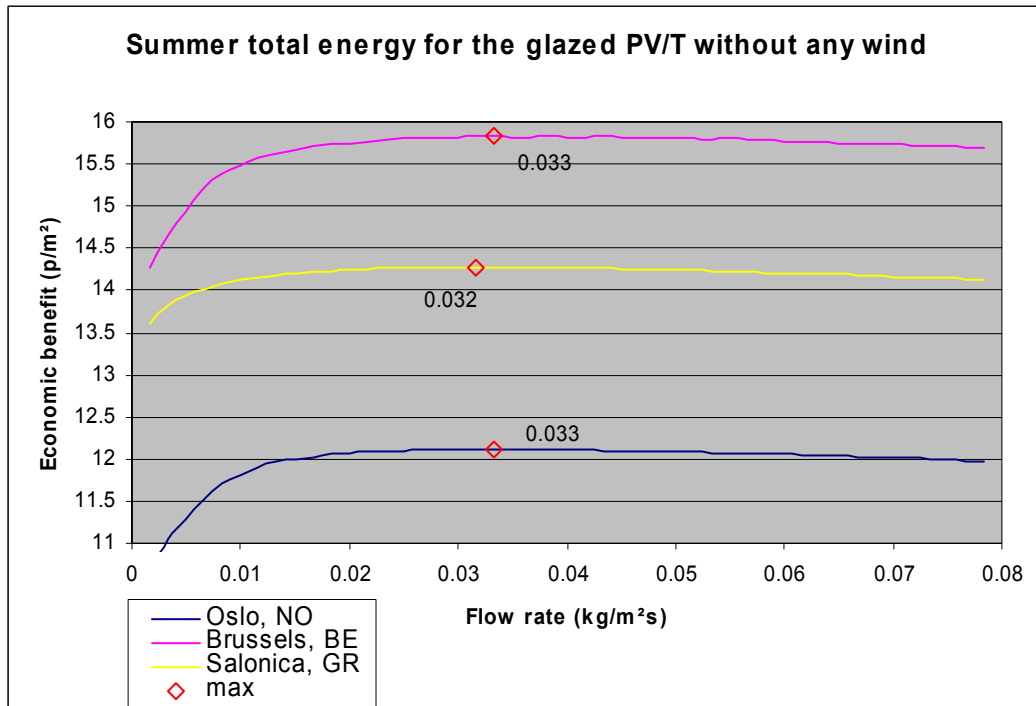
Comparing now the results from the performed simulations, a variation to the optimum flow rate can be spotted according to the latitude



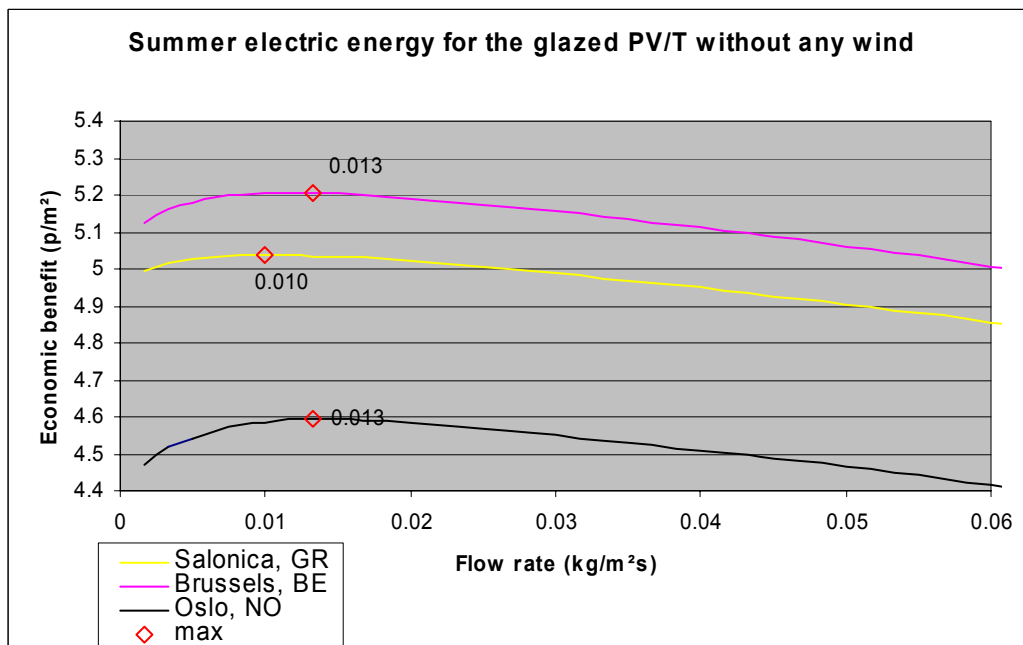
Graph 17

and climate properties, especially in the winter simulations. As observed in Graph 17 due to the higher ambient temperature and irradiation levels, the optimum flow rate gets a larger value for lower latitudes.

On the contrary, the summer simulations prove that at higher



Graph 19



Graph 18

temperatures and irradiation levels the optimum flow rate does not change. In addition, the lower latitude simulation had less economic benefit than the central latitude one. The higher irradiation and temperature levels deprive the system of keeping an energy production rate higher than the energy required rate to drive the pump. As a result the economic optimum flow rate is lower for the lower latitude during this summer simulation.

Previous studies that examined various aspects of the PV/T system have used flow rates that are in between the range of this study's results. Mattei *et al.*²⁰ studied, through simulation, the performance characteristics of such a module for France, and determined as the optimum flow rate the rate of 0.2m³/hr which is equal to 0.005kg/s. In addition to that, Tripanagnostopoulos *et al.*² used the flow rate of 0.02kg/s for their experiments. These values lie inside the boundaries of the results demonstrated above, and prove that the mathematical model and the process that has been developed is convincing.

Finally, the annual savings derived from the optimum flow rates of the above simulations, assuming 45% availability to the similar weather conditions that the simulations were performed and an exchange rate of €0.68/£, are illustrated in Table 1. In these values the installation and parts cost is not included.

	Oslo, NO	Brussels, BE	Thessaloniki, GR
Thermal & Electrical	€7.51/m ²	€9.59/m ²	€8.71/m ²
Electrical	€2.95/m ²	€4.04/m ²	€4.94/m ²

Table 1

Summary of conclusions

In order to better value the simulation results , a bullet point presentation is put together:

- As temperature and solar intensity increases, the optimum flow rate increases as well.
- As ambient temperature increases the economic benefit at the optimum flow rate for the solar-electric part decreases. On the contrary, the economic benefit increases, as irradiation levels increase.
- Low European latitude areas have less economic benefit during the summer, from such a hybrid module, than those of central European latitude. On the other hand, during the winter, low latitudes gain higher benefit.
- PV/T modules with an extra glazing layer, gain an advantage on high latitude applications, while bare (without an extra glazing layer) modules perform better in central and low latitude areas.

Areas for further study

The photovoltaic thermal concept is not new in the research literature. While other sustainable technologies are exploited, there is a vast number of people that are interested to increase the value of an existing technology, the photovoltaic power generation. As studies should continue on this area a more detailed economic analysis on the parts, installation costs and maintenance of these systems could give a more clear idea on what level they can be deployed. In addition to that, validation of a dynamic simulation model like the one discussed by Mattei *et al.*²⁰ would give researchers an easier approach to the design parameters that would improve the PV/T performance. Further investigation is also required to examine the cause of the fact that the summer simulations did not have the expected higher economic performance from the low latitude simulation. Finally, experimental

studies should be carried out to further investigate the subject of "optimum flow rate for a PV/T system". Preferably, these should be performed under different climate conditions and compare the results with this present study.

Conclusions

The concept of the photovoltaic/thermal hybrid module is studied and an investigation to its optimum flow rate conditions has been performed. To achieve that, a process, based on previous validated assumptions, has been built. The simulations performed using this process, illustrated that the flow rate increases as the ambient temperature and solar irradiation increase. This rise occurs up to the point that the rate of generated energy reaches the rate of that consumed, due to water pumping. As temperatures during the summer months reach levels that significantly reduce the PV performance, the energy available to drive the water pump decreases as well, dropping off the optimum flow rate.

²⁰ M, Mattei, C. Cristofari, A. Louche "Modeling a hybrid PV/T collector" Proceedings of the 2nd world conference and exhibition on PV solar energy conversion, Vienna, 1998

NOMENCLATURE

A_c	Collector area
A_{pv}	Area covered by the photovoltaic cells
C_p	Specific heat
D	Hydraulic diameter
F'	Collector efficiency factor
F_R	Heat removal factor
f_r	Friction factor
F_{WD}	Collector geometry factor
g	Gravitational force
h_c	Convection heat transfer coefficient between the two parallel plates
$h_{k, glass}$	Conduction heat transfer coefficient for glass
$h_{k, resin}$	Conduction heat transfer coefficient for the resin
$h_{r,a}$	Radiation heat transfer coefficient from the cover plate to the ambient
$h_{r,in}$	Radiation heat transfer coefficient between the cover and the cells
h_{wind}	Convection heat transfer coefficient relative to the wind
I	Solar irradiation
I_b	Solar beam intensity
I_d	Diffusion on a horizontal surface
I_{mp}	Current at maximum power point
k	Thermal conductivity
L	Pipes length
\dot{m}, m_w	Mass flow rate
m	Mass of water inside the system
N	Number of bends in a serpentine tube
Q_e	Energy generated by the PV panel
Q_T	Thermal energy
Q_{tank}	Energy dissipation from the storage tank

Q_U	Useful energy
R_b	The ratio of beam radiation on tilted surfaces to that on horizontal surfaces
\dot{S}	Solar energy available for the thermal system
S	Absorbed solar radiation
sunshine _hours	Daily time period that the pump is operating
T_a	Ambient temperature
T_i	Inlet temperature
T_{PV}	PV cell's temperature
T_{ref}	PV cell's reference temperature
T_w	Storage fluid temperature
U_{back}	Back loss coefficient
U_{fin}	Thermal conductance between the absorber and the fin
U_L	Loss coefficient
U_{top}	Top loss coefficient
v_f	Fluid velocity
V_{mp}	Voltage at maximum power point
α	Thermal diffusivity
α_{PV}	Absorptance of PV material
β	Angle between the horizontal and the module
η_{pump}	Pump's efficiency
η_{PV}	PV incident efficiency
η_{ref}	PV cell's efficiency under STC
η_T	Thermal efficiency
μ	Temperature coefficient
ρ	Density
ρ_g	Ground reflectance
$\tau\alpha$	Transmittance absorptance product

BIBLIOGRAPHY

- [1] Patel, Mukund "Wind and Solar power systems" 1999, New York, CRC Press
- [2] Duffie, John and Beckman, William "Solar Engineering of thermal processes" 1991, New York, John Wiley & Sons
- [3] Markvart, Tomas "Solar Electricity" 1998, Chichester, John Wiley & Sons
- [4] Mironer, Alan "Engineering Fluid Mechanics" 1994, McGraw-Hill
- [5] Holman, Jack "Heat transfer" 8th edition, 1997, McGraw-Hill
- [6] Ogata, Katsuhito "System Dynamics" 2nd edition, 1992, Prentice-Hall
- [7] Incropera, Frank and DeWitt, David "Fundamentals of heat and mass transfer" 4th edition, 1996, New York, John Wiley & Sons
- [8] MathCAD, User's guide, Mathsoft Inc.
- [9] Clarke Joseph "Energy Simulation in Building Design" 2nd edition, 2001, Butterworth-Heinemann
- [10] Twidell, John and Weir, Tony "Renewable Energy Resources" 2000, E&FN Spon

Apart from the above mentioned books and the articles documented in the endnotes of each chapter, a variety of other selected articles from the Solar Energy Journal and the proceedings of the European PV solar energy conferences in Glasgow and Vienna were consulted to acquire adequate understanding for the studied subject.

APPENDIXES

1. Material properties and constants
2. Steady state energy balance
3. System analysis
4. Optimization

APPENDIX 1

Material Properties and Constants

Stefan Boltzmann Constant $\sigma := 5.670 \cdot 10^{-8} \cdot \frac{\text{watt}}{\text{m}^2 \cdot \text{K}^4}$

Air properties at 60C (approximate average temperature between the glazing and the PV)

$$k_{\text{air}} := 0.029 \frac{\text{watt}}{\text{m} \cdot \text{K}} \quad v := 1.88 \cdot 10^{-5} \frac{\text{m}^2}{\text{s}} \quad \alpha := 2.69 \cdot 10^{-5} \frac{\text{m}^2}{\text{s}}$$

PV module properties

BP 4160 monocrystalline

$$V_{\text{mp}} := 35.4\text{V} \quad I_{\text{mp}} := 4.52\text{A} \quad L_c := 1580\text{mm} \quad W_c := 783\text{mm} \quad A_c := L_c \cdot W_c \quad A_c = 1.237\text{m}^2 \quad A_{\text{PV}} := .9 \cdot A_c$$

$$T_{\text{ref}} := (273 + 25)\text{K} \quad \mu := .05 \frac{\%}{\text{K}} \quad \eta_{\text{ref}} := \frac{V_{\text{mp}} \cdot I_{\text{mp}}}{A_{\text{PV}} \cdot I} \quad \eta_{\text{ref}} = 17.742\%$$

Typical pv-material properties

$$k_{\text{PV}} := .18 \frac{\text{watt}}{\text{m} \cdot \text{K}} \quad \delta_{\text{PV}} := 1\text{mm}$$

$$\varepsilon_{\text{PV}} := 84\% \quad \alpha_{\text{PV}} := 84\%$$

Storage tank properties (Rigid Polyester Thermoset)

$$\delta_{\text{tank}} := 30\text{mm} \quad k_{\text{tank}} := .17 \frac{\text{watt}}{\text{m} \cdot \text{K}} \quad U_{\text{tank}} := \frac{k_{\text{tank}}}{\delta_{\text{tank}}}$$

Insulation material properties

$$\delta_I := 50\text{mm} \quad k_I := 0.04 \frac{\text{watt}}{\text{m} \cdot \text{K}} \quad (\text{glass fiber } .04\text{W/mK} - \text{polyurethane } .05\text{W/mK})$$

$$U_{\text{back}} := \frac{k_I}{\delta_I}$$

Other material properties

Glass glazing

$$\rho_g := 8\% \quad \tau_g := 88\% \quad \varepsilon_g := 88\%$$

Copper pipes and absorbing plate

$$k_{\text{copper}} := 211 \frac{\text{watt}}{\text{m} \cdot \text{K}} \quad \delta_{\text{copper}} := 1\text{mm}$$

$$\delta_f := \delta_{\text{PV}} + \delta_{\text{copper}} \quad k_f := \frac{\delta_{\text{copper}}}{\delta_f} \cdot k_{\text{copper}} + \frac{\delta_{\text{PV}}}{\delta_f} \cdot k_{\text{PV}} \quad h_f := \frac{k_f}{\delta_f}$$

Transmittance - Absorptance product $\tau\alpha := \frac{\tau_g \cdot \alpha_{pv}}{1 - (1 - \alpha_{pv}) \cdot \rho_g}$

Length facing the wind direction

$$L := W_c$$

Spacing between glass and PV

$$L_{sp} := 25\text{mm}$$

Working fluid properties

Water

$$C_p := 4200 \frac{\text{J}}{\text{kg}\cdot\text{K}} \quad \rho_w := 1000 \frac{\text{kg}}{\text{m}^3} \quad k_w := 620 \cdot 10^{-3} \frac{\text{watt}}{\text{m}\cdot\text{K}} \quad \mu_w := 1000 \cdot 10^{-6} \frac{\text{N}\cdot\text{s}}{\text{m}^2}$$

APPENDIX 2

Steady State Energy Balance

Heat transfer coefficient for the wind

$$h_{\text{wind}} := \left[\max \left[5, \frac{8.6 \left(\frac{V_{\text{wind}} \cdot s}{m} \right)^{0.6}}{\left(\frac{L}{m} \right)^{0.4}} \right] \right]$$

Given (Start of the iteration solving block)

Glazing layer temperature

$$T_{\text{gl}} = T_{\text{PV}} - \frac{U_{\text{top}} \cdot (T_{\text{PV}} - T_{\text{a}})}{h_{\text{conv}} + \frac{\sigma \cdot (T_{\text{PV}} + T_{\text{gl}}) \cdot (T_{\text{PV}}^2 + T_{\text{gl}}^2)}{\frac{1}{\varepsilon_{\text{PV}}} + \frac{1}{\varepsilon_{\text{g}}} - 1}}$$

Sky temperature

$$T_{\text{sky}} := 0.05532 \cdot \left(\frac{T_{\text{a}}}{\text{K}} \right)^{1.5} \cdot \text{K}$$

Air temperature between the glazing layer and the PV

$$T_{\text{air}} = \frac{T_{\text{PV}} + T_{\text{gl}}}{2}$$

$$\text{Nu} = \left\{ \begin{array}{l} \beta' \leftarrow \frac{1}{T_{\text{air}}} \\ \text{Ra} \leftarrow \frac{g \cdot \beta' \cdot (T_{\text{PV}} - T_{\text{gl}}) \cdot L_{\text{sp}}^3}{\nu \cdot \alpha} \\ \text{Nu1a} \leftarrow \left[\sqrt[3]{\frac{\text{Ra} \cdot \cos(\beta)}{5830}} - 1 \right] \\ \text{Nu1} \leftarrow \left\{ \begin{array}{l} \text{Nu1a} \text{ if } \text{Nu1a} > 0 \\ 0 \text{ otherwise} \end{array} \right. \\ \text{Nu2a} \leftarrow \left(1 - \frac{1708}{\text{Ra} \cdot \cos(\beta)} \right) \\ \text{Nu2} \leftarrow \left\{ \begin{array}{l} \text{Nu2a} \text{ if } \text{Nu2a} > 0 \\ 0 \text{ otherwise} \end{array} \right. \\ 1 + 1.44 \cdot \left[1 - \frac{1708 \cdot (\sin(1.8 \cdot \beta))^{1.6}}{\text{Ra} \cdot \cos(\beta)} \right] \cdot \text{Nu2} + \text{Nu1} \end{array} \right.$$

$$h_{\text{conv}} = \frac{\text{Nu} \cdot k_{\text{air}}}{L_{\text{sp}}}$$

Nusset number for the estimating the convection coefficient between two parallel plates, the glazing layer and the PV.

Convection coefficient for the natural convection between the glazing area and the PV.

Top loss coefficient for one glazing layer (top) and for no glazing area (bottom)

$$U_{\text{top}} = \begin{cases} \left[\frac{1}{h_{\text{conv}} + \frac{\sigma \cdot (T_{\text{PV}} + T_{\text{gl}}) \cdot (T_{\text{PV}}^2 + T_{\text{gl}}^2)}{\frac{1}{\varepsilon_{\text{PV}}} + \frac{1}{\varepsilon_{\text{g}}} - 1}} + \frac{1}{h_{\text{wind}} \cdot \frac{\text{watt}}{\text{m}^2 \cdot \text{K}} + \sigma \cdot \varepsilon_{\text{PV}} \cdot (T_{\text{PV}} + T_{\text{sky}}) \cdot (T_{\text{PV}}^2 + T_{\text{sky}}^2)} \right]^{-1} & \text{if } N = 1 \\ \left[\frac{1}{\frac{k_{\text{PV}}}{\delta_{\text{PV}}} + \frac{1}{h_{\text{wind}} \cdot \frac{\text{watt}}{\text{m}^2 \cdot \text{K}} + \sigma \cdot \varepsilon_{\text{PV}} \cdot (T_{\text{PV}} + T_{\text{sky}}) \cdot (T_{\text{PV}}^2 + T_{\text{sky}}^2)}} \right]^{-1} & \text{otherwise} \end{cases}$$

Overall heat loss coefficient

$$U_{\text{L}} = U_{\text{top}} + U_{\text{back}}$$

Heat removal factor (F' is the fin efficiency factor)

$$F_{\text{R}} = \frac{m_{\text{w}} \cdot C_{\text{p}}}{A_{\text{c}} \cdot U_{\text{L}}} \left(1 - \exp\left(\frac{-A_{\text{c}} \cdot U_{\text{L}} \cdot F'}{m_{\text{w}} \cdot C_{\text{p}}}\right) \right) \quad F' = \frac{1}{1 + \frac{U_{\text{L}}}{h_{\text{f}}}}$$

Thermal gain for the system

Solar fraction gained from the thermal system

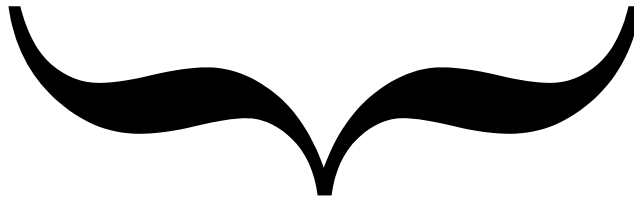
$$Q_{\text{T}} = A_{\text{c}} \cdot F_{\text{R}} \cdot [S - U_{\text{L}} \cdot (T_{\text{i}} - T_{\text{a}})] \quad S = \left(\tau \alpha - \eta_{\text{PV}} \cdot \frac{A_{\text{pv}}}{A_{\text{c}}} \right) \cdot I$$

Module temperature

Thermal system efficiency

Electrical system efficiency

$$T_{\text{PV}} = T_{\text{i}} + \frac{1 - F_{\text{R}}}{F_{\text{R}} \cdot U_{\text{L}}} \cdot \eta_{\text{T}} \cdot I \quad \eta_{\text{T}} = \frac{Q_{\text{T}}}{A_{\text{c}} \cdot I} \quad \eta_{\text{PV}} = \eta_{\text{ref}} - \mu \cdot (T_{\text{PV}} - T_{\text{ref}})$$



Simplification made to ease the iteration

$$T_{\text{PV}} = \frac{\left[\left[(-\tau \alpha \cdot F_{\text{R}} + \tau \alpha) \cdot I + (T_{\text{i}} - T_{\text{a}}) \cdot U_{\text{L}} \cdot F_{\text{R}} + T_{\text{a}} \cdot U_{\text{L}} \right] \cdot A_{\text{c}} + \left[(\eta_{\text{ref}} + \mu \cdot T_{\text{ref}}) \cdot A_{\text{pv}} \cdot F_{\text{R}} + (-\eta_{\text{ref}} - \mu \cdot T_{\text{ref}}) \cdot A_{\text{pv}} \right] \cdot I \right]}{\left[(\mu \cdot A_{\text{pv}} \cdot F_{\text{R}} - \mu \cdot A_{\text{pv}}) \cdot I + U_{\text{L}} \cdot A_{\text{c}} \right]}$$

Find($U_{\text{top}}, U_{\text{L}}, T_{\text{PV}}, F_{\text{R}}, T_{\text{gl}}, T_{\text{air}}, Nu, h_{\text{conv}}, F'$)

(End of solve block)

APPENDIX 3

System analysis

Reading data values from relative output files

$$\begin{pmatrix} \text{tot_time} \\ \text{time_init} \\ \text{mean_rad} \\ \text{mean_temp} \end{pmatrix} := \text{READPRN}("E:\text{My Documents}\text{Strathclyde}\text{Part C Thesis}\text{weather}\text{data summer low.prn}")$$

Applying the average heat loss coefficient value from the steady state model simulation

$$U_L := \text{mean} \left(\text{READPRN}("1-0\text{wall 2 wall summer low 1-0.dat}") \cdot \frac{\text{watt}}{\text{m}^2 \cdot \text{K}} \right)$$

Reading regression coefficients from weather files.

irad := "E:\My Documents\Strathclyde\Part C Thesis\weather\Thessaloniki\iradiationcoeffs low-summer.prn"

I_{coeffs} := READPRN(irad)

temp := "E:\My Documents\Strathclyde\Part C thesis\weather\temperature low summer.prn"

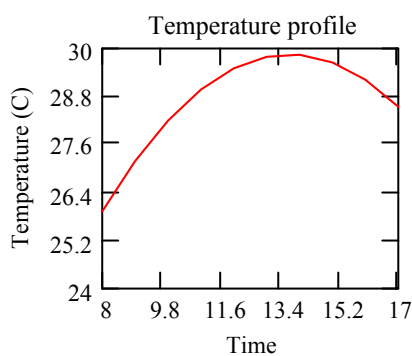
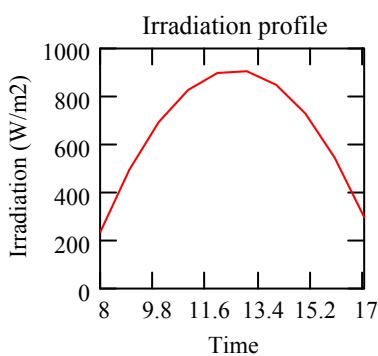
T_{coeffs} := READPRN(temp)

Radiation and temperature profile polynomials

$$I(t) := \left[I_{\text{coeffs}_0} + \sum_c I_{\text{coeffs}_c} \cdot (t)^c \right] \frac{\text{watt}}{\text{m}^2}$$

$$T_a(t) := \left[T_{\text{coeffs}_0} + \sum_c T_{\text{coeffs}_c} \cdot (t)^c \right] \text{K} + 273\text{K}$$

Plots



Tank volume

Tank area

$$m_w := 150\text{kg}$$

$$A_{\text{tank}} := \left(\frac{m_w}{1000\text{kg}} + \frac{1\% m_w}{1000\text{kg}} \right) \text{m}^2$$

Estimated average heat loss coefficients for the storage tank.

$$U_{\text{tank}} := 5 \frac{\text{watt}}{\text{m}^2 \cdot \text{K}}$$

Heat removal factor

$$F_R := 0.85$$

The differential equation solve block to determine the tank water temperature throughout the day.

Given

$$\frac{d}{dt} T_w(t) = \frac{\text{if}[A_c \cdot F_R \cdot [\tau \alpha_{\text{eff}} \cdot I(t) \cdot \text{hr} - U_L \cdot (T_w(t) - T_a(t))] > 0, A_c \cdot F_R \cdot [\tau \alpha_{\text{eff}} \cdot I(t) \cdot \text{hr} - U_L \cdot (T_w(t) - T_a(t))], 0] - U_{\text{tank}} \cdot A_{\text{tank}} \cdot (T_w(t) - T_a)}{m_w \cdot C_p}$$

Initial value

$$T_w(t_0) = 286$$

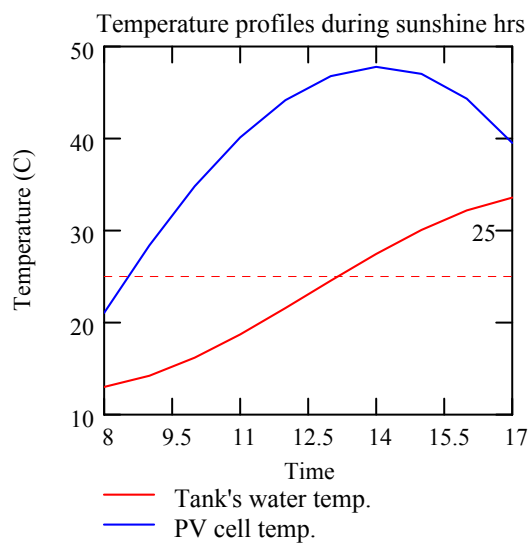
Tank water temperature

$$T_w := \text{Odesolve}(t, 100)$$

PV plate average temperature

$$T_c(t) := T_w(t) \text{K} + \frac{1 - F_R}{F_R \cdot U_L} \cdot I(t) \cdot \eta_T(t)$$

Plot



Tank's and PV module's thermal gains

$$Q_{\text{tank}}(t) := U_{\text{tank}} \cdot A_{\text{tank}} \cdot (T_{\text{w}}(t) \text{ K} - T_{\text{a}}(t))$$

$$Q_{\text{PV}}(t) := \text{if} \left[\left[A_{\text{c}} \cdot F_{\text{R}} \cdot \left[\tau \alpha_{\text{eff}} \cdot I(t) - U_{\text{L}} \cdot (T_{\text{w}}(t) \text{ K} - T_{\text{a}}(t)) \right] \right] > 0, \left[A_{\text{c}} \cdot F_{\text{R}} \cdot \left[\tau \alpha_{\text{eff}} \cdot I(t) - U_{\text{L}} \cdot (T_{\text{w}}(t) \text{ K} - T_{\text{a}}(t)) \right] \right], 0 \text{ watt} \right]$$

Usefull thermal energy

$$Q_{\text{U}} := \int_{t_0}^{t_{\text{rows}}(t)-1} Q_{\text{PV}}(t) - Q_{\text{tank}}(t) \text{ dt} \cdot \text{hr} \quad Q_{\text{U}} = 3.894 \text{ kW} \cdot \text{hr}$$

Electrical energy

$$Q_{\text{e}} := \int_{t_0}^{t_{\text{rows}}(t)-1} \left(\eta_{\text{PV}}(t) \cdot \frac{S(t)}{\alpha_{\text{PV}}} \cdot A_{\text{c}} \right) \text{ dt} \cdot \text{hr} \quad Q_{\text{e}} = 0.695 \text{ kW} \cdot \text{hr}$$

Appending results into a file for analysis

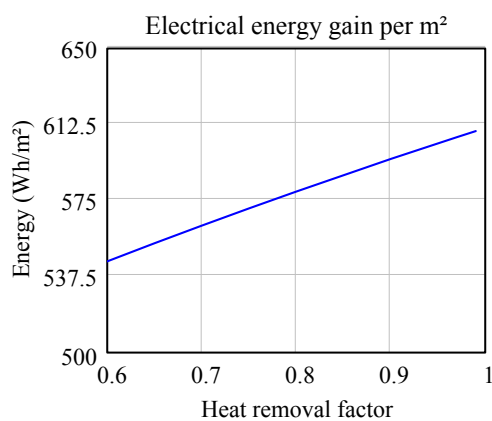
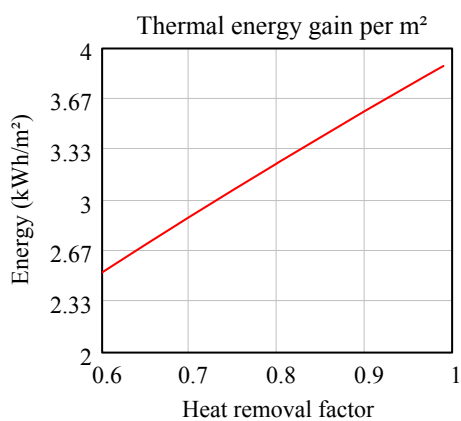
$$F_{\text{m}} := \text{augment} \left(F_{\text{R}}, \frac{Q_{\text{e}}}{\text{W} \cdot \text{hr}}, \frac{Q_{\text{U}}}{\text{W} \cdot \text{hr}} \right)$$

file := "energy vs factor low summer10.prn"

data := WRITEPRN(file, Fm) on error APPENDPRN(file, Fm)

plot := csort(data, 0)

Plotting the data



APPENDIX 4

Optimisation

Reading relevant data files

Data from the relation between the flow rate and the heat removal factor

```
data1 := "1-5\wall 2 wall summer low 1-5.dat"
```

Data from the relation between the heat removal factor and the energy gains

```
data2 := "energy vs factor low summer15.prn"
```

Reading the data from the above files

```
g1 := READPRN(data1)      g2 := READPRN(data2)
```

Extracting the heat removal factor from the data files

```
FR := Extract(g1<1>, c)
```

Creating an array representing the flow rate

```
i := 1..49
```

```
mwi := 0 ·  $\frac{\text{kg}}{\text{s}}$  + .002 · i ·  $\frac{\text{kg}}{\text{s}}$ 
```

Pumping

Determination of the energy surcharge due to pumping

Hydraulic diameter

$$D := 10\text{mm}$$

Pipe length (approx)

$$L := 1\text{m}$$

Water properties at 45 C

$$\text{Pr} := 4 \quad k := 637 \cdot 10^{-3} \frac{\text{watt}}{\text{m} \cdot \text{K}}$$

Cross sectional area

$$A := \left(\frac{D}{2}\right)^2 \pi$$

head := 1m

$$\rho_w := 1000 \frac{\text{kg}}{\text{m}^3} \quad \mu := 600 \cdot 10^{-6} \frac{\text{N} \cdot \text{s}}{\text{m}^2}$$

Pump efficiency

$$\eta_{\text{pump}} := 18.6\%$$

Reynolds number

$$\text{Re}_i := \frac{4 m_{w_i}}{\mu \cdot D \cdot \pi}$$

Fluid velocity

$$u_i := \frac{m_{w_i}}{A \cdot \rho_w}$$

Friction factor

$$f_i := \begin{cases} \frac{64}{\text{Re}_i} & \text{if } \text{Re}_i \leq 2300 \\ \left(0.79 \cdot \ln(\text{Re}_i) - 1.64\right)^{-2} & \text{otherwise} \end{cases}$$

Pumping energy needs

$$P_{\text{pump}_i} := m_{w_i} \cdot \left[\text{g.head} + f_i \cdot \frac{L}{D} \cdot \frac{(u_i)^2}{2} \right] \cdot \frac{1}{\eta_{\text{pump}}} \cdot \text{tot.time hr}$$

Regression

Creating polynomial functions of the energy gains and the heat removal factor.

$$X := g2^{(0)} \quad Y := g2^{(1)} \quad Y_2 := g2^{(2)}$$

$$n := \text{rows}(g2)$$

Enter degree of polynomial to fit:

$$k := 1$$

Number of data points:

$$n = 10$$

$$z := \text{regress}(X, Y, k)$$

$$z_2 := \text{regress}(X, Y_2, k)$$

Polynomial fitting function:

$$\text{fit}(x) := \text{interp}(z, X, Y, x)$$

$$\text{fit}_2(x) := \text{interp}(z_2, X, Y_2, x)$$

$$\text{coeffs} := \text{submatrix}(z, 3, \text{length}(z) - 1, 0, 0)$$

$$\text{coeffs}_2 := \text{submatrix}(z_2, 3, \text{length}(z_2) - 1, 0, 0)$$

Coefficients:

$$\text{coeffs}^T = (592.504 \quad 141.013)$$

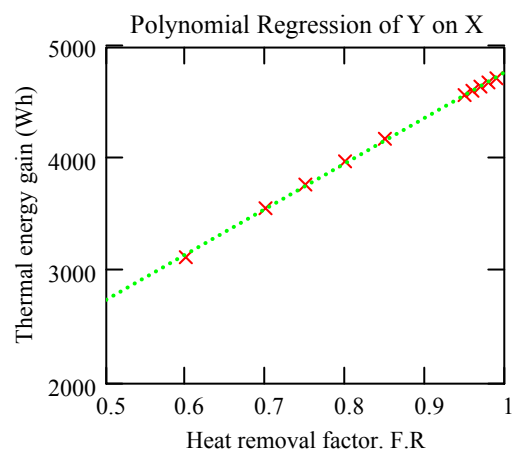
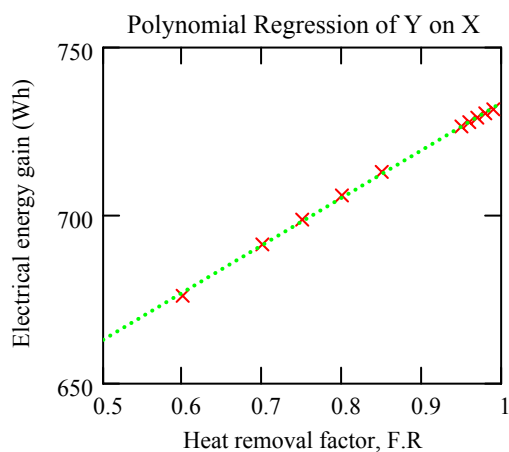
$$\text{coeffs}_2^T = (719.081 \quad 4.058 \times 10^3)$$

$$R^2: \frac{\sum (\text{fit}(X) - \text{mean}(Y))^2}{\sum (Y - \text{mean}(Y))^2} = 0.999$$

$$\frac{\sum (\text{fit}_2(X) - \text{mean}(Y_2))^2}{\sum (Y_2 - \text{mean}(Y_2))^2} = 0.999$$

Degrees of freedom: $n - k - 1 = 8$ $c := 1..k$

Plots



Relations of the energy gains as a function of the heat removal factor

$$Q_T(FR) := \left[\text{coeffs}_{2_0} + \sum_c \text{coeffs}_{2_c} \cdot (FR)^c \right] \cdot W \cdot \text{hr}$$

$$Q_e(FR) := \left[\text{coeffs}_0 + \sum_c \text{coeffs}_c \cdot (FR)^c \right] W \cdot \text{hr}$$

Application of the economic sensitivity factors

$$\text{total} := Q_e(FR) \cdot 7 \cdot \frac{p}{\text{kW} \cdot \text{hr}} + Q_T(FR) \cdot 2 \cdot \frac{p}{\text{kW} \cdot \text{hr}} - 7 \cdot \frac{p}{\text{kW} \cdot \text{hr}} \cdot P_{\text{pump}}$$

$$\text{electric} := Q_e(FR) \cdot 7 \cdot \frac{p}{\text{kW} \cdot \text{hr}} - 7 \cdot \frac{p}{\text{kW} \cdot \text{hr}} \cdot P_{\text{pump}}$$

$$Fm := \text{augment} \left(\frac{\text{total}}{p}, \frac{m_w \cdot s}{\text{kg} \cdot 1.2} \right)$$

$$Fm2 := \text{augment} \left(\frac{\text{electric}}{p}, \frac{m_w \cdot s}{\text{kg} \cdot 1.2} \right)$$

Determination of the maximum value, which is the optimum condition

$$Xm_w := \max \left(\text{lookup} \left(\frac{\max(\text{total})}{p}, Fm^{(0)}, Fm^{(1)} \right) \right) \frac{\text{kg}}{\text{s}}$$

$$X2m_w := \max \left(\text{lookup} \left(\frac{\max(\text{electric})}{p}, Fm2^{(0)}, Fm2^{(1)} \right) \right) \frac{\text{kg}}{\text{s}}$$

$$Y_p := \max(\text{total})$$

$$Y2_p := \max(\text{electric})$$

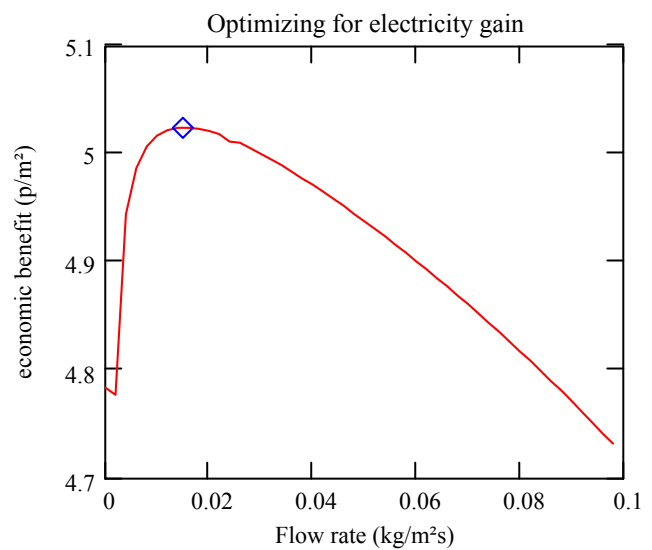
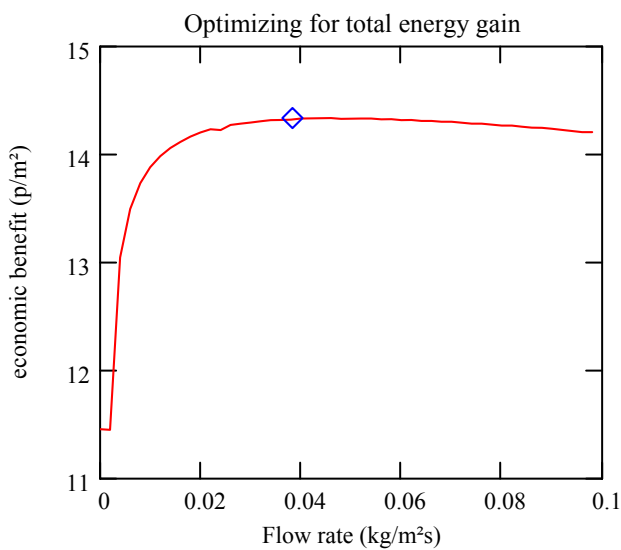
$$Y_p = 14.337 p$$

$$Y2_p = 5.025 p$$

$$Xm_w = 0.038 \frac{\text{kg}}{\text{s}}$$

$$X2m_w = 0.015 \frac{\text{kg}}{\text{s}}$$

Plotting the results



NOTE: the blue diamond represents the optimum condition